filament networks with alteration of cell shape and nuclear integrity. *J Invest Dermatol* 108:179–87

Deshpande R, Woods TL, Fu J *et al.* (2000) Biochemical characterization of S100A2 in human keratinocytes: subcellular localization, dimerization, and oxidative cross-linking. *J Invest Dermatol* 115: 477–85

Donato R (2001) S100: a multigenic family of calcium-modulated proteins of the EF-hand type with intracellular and extracellular functional roles. *Int J Biochem Cell Biol* 33:637–68

Eckert RL, Broome AM, Ruse M *et al.* (2004) S100 proteins in the epidermis. *J Invest Dermatol* 123:23–33

Elias PM, Ahn SK, Denda M *et al.* (2002) Modulations in epidermal calcium regulate the expression of differentiation-specific markers. *J Invest Dermatol* 119:1128–36

Han SY, Gai W, Yancovitz M *et al.* (2008) Nucleofection is a highly effective gene transfer technique for human melanoma cell lines. *Exp Dermatol* 17:405–11

Hohl D, Mehrel T, Lichti U *et al.* (1991) Characterization of human loricrin. Structure and function of a new class of epidermal cell envelope proteins. *J Biol Chem* 266:6626–36

Hudson JR Jr, Dawson EP, Rushing KL *et al.* (1997) The complete set of predicted genes from Saccharomyces cerevisiae in a readily usable form. *Genome Res* 7:1169–73

Ishida-Yamamoto A, Hohl D, Roop DR *et al.* (1993) Loricrin immunoreactivity in human skin: localization to specific granules (L-granules) in acrosyringia. *Arch Dermatol Res* 285:491–8

Ishida-Yamamoto A, Takahashi H, Presland RB *et al.* (1998) Translocation of profilaggrin N-terminal domain into keratinocyte nuclei with fragmented DNA in normal human skin and loricrin keratoderma. *Lab Invest* 78:1245–53

Kalinin A, Marekov LN, Steinert PM (2001) Assembly of the epidermal cornified cell envelope. *J Cell Sci* 114:3069–70

Kalinin AE, Kajava AV, Steinert PM (2002) Epithelial barrier function: assembly and structural features of the cornified cell envelope. *Bioessays* 24:789–800

Koch PJ, de Viragh PA, Scharer E *et al.* (2000) Lessons from loricrin-deficient mice: compensatory mechanisms maintaining skin barrier function in the absence of a major cornified envelope protein. *J Cell Biol* 151: 389–400

Kuechle MK, Thulin CD, Presland RB *et al.* (1999) Profilaggrin requires both linker and filaggrin peptide sequences to form granules: implications for profilaggrin processing *in vivo*. *J Invest Dermatol* 112:843–52

Mauro T, Bench G, Sidderas-Haddad E *et al.* (1998) Acute barrier perturbation abolishes the Ca^{2+} and K^{+} gradients in murine epidermis: quantitative measurement using PIXE. *J Invest Dermatol* 111:1198–201

Mehrel T, Hohl D, Rothnagel JA *et al.* (1990) Identification of a major keratinocyte cell envelope protein, loricrin. *Cell* 61:1103–12

Mildner M, Jin J, Eckhart L *et al.* (2010) Knockdown of filaggrin impairs diffusion barrier function and increases UV sensitivity in a human skin model. *J Invest Dermatol* 130:2286–94

Miyake S, Makimura M, Kanegae Y *et al.* (1996) Efficient generation of recombinant adenoviruses using adenovirus DNA-terminal protein complex and a cosmid bearing the full-length virus genome. *Proc Natl Acad Sci USA* 93:1320–4

Okada M, Hatakeyama T, Itoh H *et al.* (2004) S100A1 is a novel molecular chaperone and a member of the Hsp70/Hsp90 multichaperone complex. *J Biol Chem* 279:4221–33

O'Shaughnessy RF, Welti JC, Cooke JC *et al.* (2007) AKT-dependent HspB1 (Hsp27) activity in epidermal differentiation. *J Biol Chem* 282: 17297–305

Pearton DJ, Dale BA, Presland RB (2002) Functional analysis of the profilaggrin N-terminal peptide: identification of domains that regulate nuclear and cytoplasmic distribution. *J Invest Dermatol* 119:661–9

Pearton DJ, Nirunsuksiri W, Rehemtulla A *et al.* (2001) Proprotein convertase expression and localization in epidermis: evidence for multiple roles and substrates. *Exp Dermatol* 10:193–203

Presland RB, Bassuk JA, Kimball JR *et al.* (1995) Characterization of two distinct calcium-binding sites in the amino-terminus of human profilaggrin. *J Invest Dermatol* 104:218–23

Presland RB, Haydock PV, Fleckman P *et al.* (1992) Characterization of the human epidermal profilaggrin gene. Genomic organization and identification of an S-100-like calcium binding domain at the amino terminus. *J Biol Chem* 267:23772–81

Presland RB, Kimball JR, Kautsky MB *et al.* (1997) Evidence for specific proteolytic cleavage of the *N*-terminal domain of human profilaggrin during epidermal differentiation. *J Invest Dermatol* 108:170–8

Robinson NA, Lapic S, Welter JF *et al.* (1997) S100A11, S100A10, annexin I, desmosomal proteins, small proline-rich proteins, plaminogen activator inhibitor-2, and involucrin are components of the cornified envelope of cultured human epidermal keratinocytes. *J Biol Chem* 272:12035–46

Ruse M, Lambert A, Robinson N *et al.* (2001) S100A7, S100A10, and S100A11 are transglutaminase substrates. *Biochemistry* 40:3167–73

Sandilands A, Sutherland C, Irvine AD *et al.* (2009) Filaggrin in the frontline: role in skin barrier function and disease. *J Cell Sci* 122:1285–94

Steinert PM, Marekov LN (1995) The proteins elafin, filaggrin, keratin intermediate filaments, loricrin, and small proline-rich proteins 1 and 2 are isodipeptide cross-linked components of the human epidermal cornified cell envelope. *J Biol Chem* 270:17702–11

Steinert PM, Marekov LN (1997) Direct evidence that involucrin is a major early isopeptide cross-linked component of the keratinocyte cornified cell envelope. *J Biol Chem* 272:2021–30

Yoneda K, Akiyama M, Morita K *et al.* (1998) Expression of transglutaminase 1 in human hair follicles, sebaceous glands and sweat glands. *Br J Dermatol* 138:37–44

Yoneda K, Demitsu T, Manabe M *et al.* (2010a) Expression of wild-type, but not mutant, loricrin causes programmed cell death in HaCaT keratinocytes. *J Dermatol* 37:956–64

Yoneda K, Demitsu T, Nakai K *et al.* (2010b) Activation of vascular endothelial growth factor receptor 2 in a cellular model of loricrin keratoderma. *J Biol Chem* 285:16184–94

Yoneda K, Fujimoto T, Imamura S *et al.* (1990a) Distribution of fodrin in the keratinocyte *in vivo* and *in vitro*. *J Invest Dermatol* 94:724–9

Yoneda K, Fujimoto T, Imamura S *et al.* (1990b) Fodrin is localized in the cytoplasm of keratinocytes cultured in low calcium medium: immunoelectron microscopic study. *Acta Histochem Cytochem* 23:139–48

Yoneda K, Furukawa T, Zheng YJ *et al.* (2004) An autocrine/paracrine loop linking keratin 14 aggregates to tumor necrosis factor alpha-mediated cytotoxicity in a keratinocyte model of epidermolysis bullosa simplex. *J Biol Chem* 279:7296–303

Yoneda K, Hohl D, McBride OW *et al.* (1992a) The human loricrin gene. *J Biol Chem* 267:18060–6

Yoneda K, McBride OW, Korge BP *et al.* (1992b) The cornified cell envelope: loricrin and transglutaminases. *J Dermatol* 19:761–4

Yoneda K, Steinert PM (1993) Overexpression of human loricrin in transgenic mice produces a normal phenotype. *Proc Natl Acad Sci USA* 90:10754–8

Zhang T, Woods TL, Elder JT (2002) Differential responses of S100A2 to oxidative stress and increased intracellular calcium in normal, immortalized, and malignant human keratinocytes. *J Invest Dermatol* 119:1196–201

Am J Physiol Cell Physiol 304: C790–C800, 2013.
First published February 20, 2013; doi:10.1152/ajpcell.00268.2012.

Dexamethasone induces caveolin-1 in vascular endothelial cells: implications for attenuated responses to VEGF

Junsuke Igarashi,[1] Takeshi Hashimoto,[1] Kazuyo Shoji,[2] Kozo Yoneda,[2] Ikuko Tsukamoto,[3] Tetsuya Moriue,[2] Yasuo Kubota,[2] and Hiroaki Kosaka[1]

[1]*Department of Cardiovascular Physiology, Kagawa University, Kagawa, Japan;* [2]*Department of Dermatology, Kagawa University, Kagawa, Japan; and* [3]*Department of Pharmaco-Bio-Informatics, Faculty of Medicine, Kagawa University, Kagawa, Japan*

Submitted 10 August 2012; accepted in final form 14 February 2013

Igarashi J, Hashimoto T, Shoji K, Yoneda K, Tsukamoto I, Moriue T, Kubota Y, Kosaka H. Dexamethasone induces caveolin-1 in vascular endothelial cells: implications for attenuated responses to VEGF. *Am J Physiol Cell Physiol* 304: C790–C800, 2013. First published February 20, 2013; doi:10.1152/ajpcell.00268.2012.—Steroids exert direct actions on cardiovascular cells, although underlying molecular mechanisms remain incompletely understood. We examined if steroids modulate abundance of caveolin-1, a regulatory protein of cell-surface receptor pathways that regulates the magnitudes of endothelial response to vascular endothelial growth factor (VEGF). Dexamethasone, a synthetic glucocorticoid, induces caveolin-1 at both levels of protein and mRNA in a time- and dose-dependent manner in pharmacologically relevant concentrations in cultured bovine aortic endothelial cells. Aldosterone, a mineralocorticoid, but not the sex steroids 17β-estradiol, testosterone, or progesterone, elicits similar caveolin-1 induction. Caveolin-1 induction by dexamethasone and that by aldosterone were abrogated by RU-486, an inhibitor of glucocorticoid receptor, and by spironolactone, a mineralocorticoid receptor inhibitor, respectively. Dexamethasone attenuates VEGF-induced responses at the levels of protein kinases Akt and ERK1/2, small-G protein Rac1, nitric oxide production, and migration. When induction of caveolin-1 by dexamethasone is attenuated either by genetically by transient transfection with small interfering RNA or pharmacologically by RU-486, kinase responses to VEGF are rescued. Dexamethasone also increases expression of caveolin-1 protein in cultured human umbilical vein endothelial cells, associated with attenuated tube formation responses of these cells when cocultured with normal fibroblasts. Immunohistochemical analyses revealed that intraperitoneal injection of dexamethasone induces endothelial caveolin-1 protein in thoracic aorta and in lung artery in healthy male rats. Thus steroids functionally attenuate endothelial responses to VEGF via caveolin-1 induction at the levels of signal transduction, migration, and tube formation, identifying a novel point of cross talk between nuclear and cell-surface receptor signaling pathways.

receptors; signal transduction; growth factors; endothelial function; angiogenesis

STEROID HORMONES THAT ACT through nuclear glucocorticoid, mineralocorticoid, and sex steroid receptors play essential roles in the maintenance of animal body homeostasis. In pathophysiological contexts, agonists for these steroid receptors are capable of exerting direct actions on cardiovascular cells, besides modulating water balance and blood pressure. For example, glucocorticoid receptor (GR) agonists downregulate endothelial nitric oxide synthase (eNOS) expression in rodent blood vessels (38) and in cultured endothelial cells (39). Clinically, hypercortisolemia in Cushing's syndrome is correlated with higher overall cardiovascular risk (26, 35) and with attenuated endothelium-dependent flow-mediated vasodilation responses in forearm arteries (1, 4). Mineralocorticoid receptor (MR) agonists also exert direct cardiovascular actions, for example, by decreasing glucose-6-phosphate dehydrogenase activity of endothelial cells (20) or by inducing eNOS "uncoupling" (28). It has clinically been known that patients suffering from primary aldosteronism exhibit a cardiovascular complication rate out of proportion to blood pressure levels seen in those suffer from essential hypertension (6). In contrast, a sex steroid 17β-estradiol increases eNOS at the levels of enzyme activity and mRNA and protein expression levels, leading to favorable outcomes on the vasculature (17). Cardiovascular actions of steroid receptor agonists may also be related to the modulation of angiogenesis, formation of new blood vessels from the preexisting ones. For example, inhaled corticosteroid effectively attenuates pathological angiogenesis in chronic airway diseases (40). Addition of corticosteroid to infantile hemangioma-derived stem cells suppresses vascular endothelial growth factor (VEGF) production, thereby leading to attenuated tumor growth in vivo (13). VEGF represents a well-characterized polypeptide growth factor acting through specific receptor tyrosine kinases expressed on the endothelial cell surface, leading to numerous responses. However, how steroids may regulate functions of vascular endothelial cells, including those modulated by VEGF, has remained incompletely understood.

In vascular endothelium, plasmalemmal caveolae, small and flask-shaped invaginations, serve as key signal transducing microdomains (30). These microdomains are enriched in various endothelial signaling proteins, including receptors such as VEGF receptor 2 (VEGFR2), protein kinases such as Akt as well as MAP kinases ERK1/2, and effector molecules such as eNOS. Caveolins are the constituent proteins of caveolae that interact with and modulate functions of caveolae-targeted proteins (30). It appeared interesting to us that some of the steroids influence the abundance of caveolin-1 isoform. For example, progesterone and testosterone increase caveolin-1 expression in breast (31) and prostate (22) cancer cells, respectively. Caveolin-1 is upregulated by the GR agonist dexamethasone in rat-derived lung epithelial cell lines (2). We therefore examined hypotheses that steroids modulate expression levels of caveolin-1 and that induction of caveolin-1 by steroids is associated with perturbed endothelial responses to VEGF.

Address for reprint requests and other correspondence: J. Igarashi, 1750-1 Ikenobe, Miki-Cho, Kita-Gun, Kagawa 761-0793, Japan (e-mail: igarashi@med.kagawa-u.ac.jp).

MATERIALS AND METHODS

Reagents. Antibodies and related compounds were commercially obtained as follows: anti-caveolin-1, anti-eNOS, and anti-ERK1/2 monoclonal antibodies were from BD Biosciences (San Jose, CA); anti-phospho VEGFR2 antibodies (Tyr1175), anti-phospho-Akt antibody (Ser473), anti-Akt polyclonal antibody, anti-phospho-eNOS antibody (Ser1179), and anti-phospho-ERK1/2 antibody (Thr202/Tyr204) were from Cell Signaling Technologies (Beverly, MA). Polyclonal antibodies directed to actin and to von Willebrand factor (vWF) were from Santa Cruz (Santa Cruz, CA). SuperBlock reagents, SuperSignal substrates for chemiluminescence detection, Restore Western Blot Stripping Buffer, and secondary antibodies conjugated with horseradish peroxidase were from Pierce (Rockford, IL). FITC-conjugated antibody to rabbit IgG, Cy3-conjugated streptavidin, and biotin-conjugated anti-mouse IgG were from DAKO (Glostrup, Denmark). TO-PRO 3 was from Invitrogen.

Bovine aortic endothelial cells (BAECs) were obtained from Cell Systems (Kirkland, WA). DMEM, LipofectAMINE 2000, and OptiMEM were from Invitrogen (Carlsbad, CA). FBS was purchased from Hyclone (Logan, CT). Human umbilical vein endothelial cells (HUVEC), HuMedia-EG2 culture medium, and tubule staining kit for CD31 were obtained from Kurabo (Osaka, Japan). Protease Inhibitor Cocktail III was from Merck (Whitehouse Station, NJ). An angiogenesis kit that contained a coculture system of HUVEC and normal human fibroblasts, supplemented with culture medium and accessory reagents, was also from Kurabo. RNeasy mini columns were from Qiagen (Valencia, CA). Taq DNA polymerase was from Promega (Madison, WI). The Rac1 activity assay kit was from Cytoskeleton (South Acoma, CO). An automated HPLC system ENO-20 was from Eicom (Kyoto, Japan). The CytoSelect 24-well cell migration assay kit (8 μm, Colorimetric Format) was from Cell Biolabs (San Diego, CA). Male Wister rats (8-wk-old) were obtained from Japan SLC (Shizuoka, Japan). A tissue-freezing medium, Tissue Tek OTC compound, was from Sakura Finetechnical (Tokyo, Japan). Protein concentration was determined by a protein assay bicinchoninate kit from Nacalai Tesque (Kyoto, Japan). All materials were from Sigma (St. Louis, MO) unless otherwise stated.

Cell culture and drug treatment. BAEC and HUVEC were maintained in culture as described previously (14, 36). HUVEC were used between passages 3 and 6. Steroids and steroid receptor antagonists were resolved into ethanol and were stored at −80°C. After reaching subconfluence, both cells were cultured in medium containing 1% of FBS for 2 days together with various drugs before being used for experiments. The final concentration of solvents did not exceed 0.1%.

RNA preparation and amplification by real-time quantitative RT-PCR. Total RNA was isolated from BAEC using the RNeasy mini column (Qiagen) (15). One microgram of total RNA was transcribed into cDNA using random hexamer and reverse transcriptase in a total volume of 20 μl. The reverse transcription was performed at 37°C for 90 min and then at 70°C for 15 min. Quantitative RT-PCR was performed by using SYBR Premix Ex Taq II system (Takara Biotechnology Shiga, Japan) and melting curve analysis using StepOne Plus Real-time PCR system (Applied Biosystems) with 18S rRNA as a reference gene. We used the Perfect real-time supporting system (Takara) to design primers specific to bovine caveolin-1 (primer set ID: BA050199) and 18S rRNA (primer set ID: BA030502). After an initial denaturation at 95°C for 30 s, amplification was performed by denaturation at 94°C for 10 s and annealing and extension at 60°C for 40 s for 50 cycles. The quantities of amplified products were monitored directly by measuring the increase of the dye intensity of the SYBR Green II (Takara) and the ROX Reference Dye (Takara). The copy number in each PCR product was defined based on a standard curve. A calibration curve was constructed by plotting the PCR threshold cycle number at which the fluorescent signal generated during the replication process passes above a threshold value against known amounts of cDNA. Caveolin-1 mRNA expression levels were normalized with 18S rRNA mRNA level.

Immunoblot analyses. Immunoblot analyses were performed as described previously (15). After being washed with ice-cold PBS, cells were harvested and lysed into cell lysis buffer containing 20 mM Tris pH 7.5, 1 mM EDTA, 1 mM EGTA, 1% Triton X-100, 150 mM NaCl, 1 mM Na_3VO_4, 2.5 mM sodium pyrophosphate, 1 mM β-glycerophosphate, and a mixture of protease inhibitors. Proteins were denatured, size-fractionated on sodium dodecyl sulfate polyacrylamide gels, and transferred to nitrocellulose membranes. The resulting membranes were blocked and incubated with various primary antibodies, followed by incubation with corresponding horseradish peroxidase-conjugated secondary antibodies, performed in TBS (pH 7.4) supplemented with 0.1% Tween-20. Immunoreactive signals were visualized using Pierce SuperSignal substrates for chemiluminescence detection with exposure to standard X-ray films (Fuji, Tokyo, Japan). In some experiments, antibodies used in the immunoblot analyses were removed from membranes using Restore Western Blot Stripping Buffer and reprobed with different antibodies.

Isolation of caveolae-enriched fractions. Caveolae-enriched fractions were separated by using ultracentrifugation with a discontinuous sucrose gradient system essentially as previously described (15, 33). Briefly, BAEC from two 100-mm dishes were scraped together into 2 ml of "carbonate buffer" containing 500 mM sodium carbonate (pH 11), 25 mM 2-(N-morpholino)ethanesulfonic acid, and 150 mM NaCl, and the cells were homogenized and sonicated. After an aliquot of whole cell lysate had been saved, the resulting cell suspension was brought to 45% sucrose (wt/vol) by addition of 2 ml of carbonate buffer containing 90% sucrose and placed at the bottom of a 12-ml ultracentrifuge tube. A discontinuous gradient was formed above the 45% sucrose bed by addition of 4 ml each of 35 and 5% sucrose solutions prepared in carbonate buffer. After centrifugation using a RPS40T rotor (Hitachi, Tokyo, Japan), 12 × 1 ml fractions were collected starting at the top of each gradient. An equal volume of each fraction was analyzed by SDS-PAGE and immunoblotting.

Transfection with small interfering RNA. BAEC were transiently transfected with 1 nM of small interfering RNA (siRNA; Ref. 15). Sequences of control and caveolin-1-specific siRNA were exactly as described previously (12, 15). Five hours after transfection, cells were recovered in a growth medium overnight. Then, they were incubated for 48 h in medium containing 1% FBS, together with either dexamethasone or vehicle.

Rac1 activity assay. Rac1 activity in BAEC was assessed as described previously (15) using a commercially available pull-down assay kit, in which GTP-bound (activated) form of Rac1 was precipitated using beads conjugated with the glutathione *S*-transferase-tagged p21-binding domain of p21 activated kinase I.

Measurement of nitrite levels in culture media. Release of nitric oxide from BAEC for 6 min after addition of VEGF was examined by measurement of nitrite accumulation in the phenol red-free culture media as described (14). The degrees of nitrite accumulation were expressed as picomoles per milligrams of protein per minute.

Cell migration assay. The migration assay used a commercially available assay kit (15). Briefly, BAEC were tripsinized and seeded onto an insert membrane in medium containing 0.4% FBS. Cells that had migrated across the membranes toward chemoattractants were stained with a blue-color dye. They were then dissolved into a lysis solution and subjected to quantification by measuring the optical density at 560 nm.

Tube formation assay. The tube formation activity of cultured endothelial cells was assessed using a commercially available coculture system of HUVEC with normal human fibroblasts as described previously (36). Ten days following incubation periods with dexamethasone (10 μM) or vehicle, endothelial cells were stained and identified with an anti-CD-31 antibody. The area of the formed tube was measured by the ImageJ program. Four pictures from each well

were provided for the estimation. Culture media and reagents were exchanged every 3 days during the assay.

Animal studies and immunofluorescence microscopy. Immunostaining was performed as described previously (41). Twelve of the 8-wk-old male Wistar rats were housed one rat per cage with temperature and light control (25°C and 12:12-h light-dark cycle). Six each of them were intraperitoneally injected with dexamethasone (0.1 mg·kg body wt^{-1}·day^{-1}) or equivalent volume of ethanol in every morning, respectively. They were killed exactly 48 h after the initial dexamethasone administration using pentobarbital (50 mg/kg body wt ip injection). All rat lung and descending aorta tissues were embedded in a tissue-freezing medium and frozen in liquid nitrogen. Cryostat sections were incubated with primary antibodies overnight at 4°C, and the immunoreactive signal was detected with FITC-conjugated antibody to rabbit IgG or a combination of Cy3-conjugated streptavidin and biotin-conjugated anti-mouse IgG. TO-PRO-3 was used for nuclear detection. Immunofluorescent images were viewed with LSM 700 confocal laser microscope (Carl Zeiss, Jena, Germany). Immunoreactive signals corresponding to endothelial caveolin-1 in a given slice derived from either thoracic aorta or from lung artery were captured using a fluorescent microscope BioRevo BZ9000 (Keyence, Tokyo, Japan) and were quantified using the Keyence software, Dynamic Cell Count. These experimental protocols conformed to the *Guide for the Care and Use of Laboratory Animals*, published by the National Institutes of Health (NIH Publication No. 85–23, revised 1996) and were approved by the Institutional Animal Care and Use Committee of Kagawa University.

Other methods. All cellular experiments were performed at least three times. Mean values for individual experiments are expressed as means ± SE. Statistical differences were analyzed by ANOVA followed by Scheffé's *F* test or by Student's *t*-test where appropriate using Statcel3 (OMS, Saitama, Japan). A P value <0.05 was considered statistically significant.

RESULTS

We started our exploration by treating BAEC, an archetypal model of endothelial cell culture, with dexamethasone, a synthetic GR agonist. Quantitative RT-PCR assays revealed that dexamethasone (for 48 h) led to dose (Fig. 1*A*)- and time (Fig. 1*B*)-dependent increases in caveolin-1 mRNA abundance. We also subjected the same cDNA templates to conventional semiquantitative RT-PCR assays and obtained similar results that caveolin-1 mRNA abundance was augmented with dexamethasone treatment (data not shown). Additionally, we noted that dexamethasone did not alter the amounts of BAEC transcripts that encode GAPDH. We next studied the effects of dexamethasone on caveolin-1 protein amounts. Dexamethasone induced a dose-dependent upregulation of caveolin-1 at a level of protein expression (Fig. 2). We tested the effects of several other steroid receptor agonists and found that aldosterone, a MR agonist, but not the sex steroids 17β-estradiol, testosterone, or progesterone, elicited induction of caveolin-1 protein albeit to a lesser extent than does dexamethasone (Fig. 2). Not only dexamethasone but also cortisol and corticosterone, which represent endogenously produced glucocorticoids in various animal species (10), similarly upregulated caveolin-1 abundance in BAEC (data not shown).

Because caveolin-1 protein undergoes a variety of posttranslational modifications including oligomerization and translocates to caveolae microstructures of peripheral plasma membrane (reviewed in Ref. 7), it was of interest to explore whether or not caveolin-1 is properly targeted to caveolae-enriched fractions even after being upregulated by dexamethasone. For

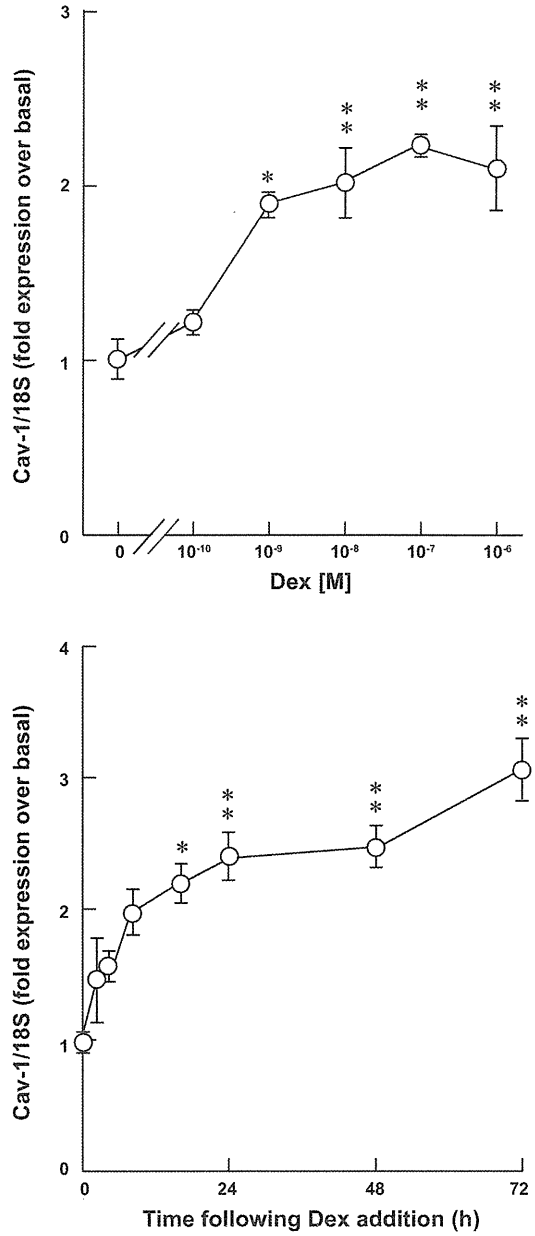

Fig. 1. Effects of dexamethasone on caveolin-1 mRNA abundance in bovine aortic endothelial cells (BAECs). Shown are the results of quantitative (q)RT-PCR assays. BAEC were treated with dexamethasone (Dex) either at the indicated concentration for 48 h (*A*) or at 1 μM for the times indicated (*B*), followed by RNA isolation. Reverse-transcribed template cDNA samples were subjected to qRT-PCR using the primers specific to bovine caveolin-1 (Cav-1) as well as 18S. Each data point represents the fold increase in transcript expression levels of Cav-1 relative to those of 18S, normalized to the values obtained from the cells before stimulation with Dex. $*P < 0.05$ and $**P < 0.01$ vs. cells treated with vehicle alone; $n = 4$ and 6 in *A* and *B*, respectively.

this sake, we performed a well-established detergent-free subcellular fractionation protocol with a discontinuous sucrose density system (33) to analyze BAEC lysates (15) with or without dexamethasone. The results indicate that caveolin-1 signals were detected only at the interface between 5 and 35% sucrose solutions, which represent caveolae-enriched fractions

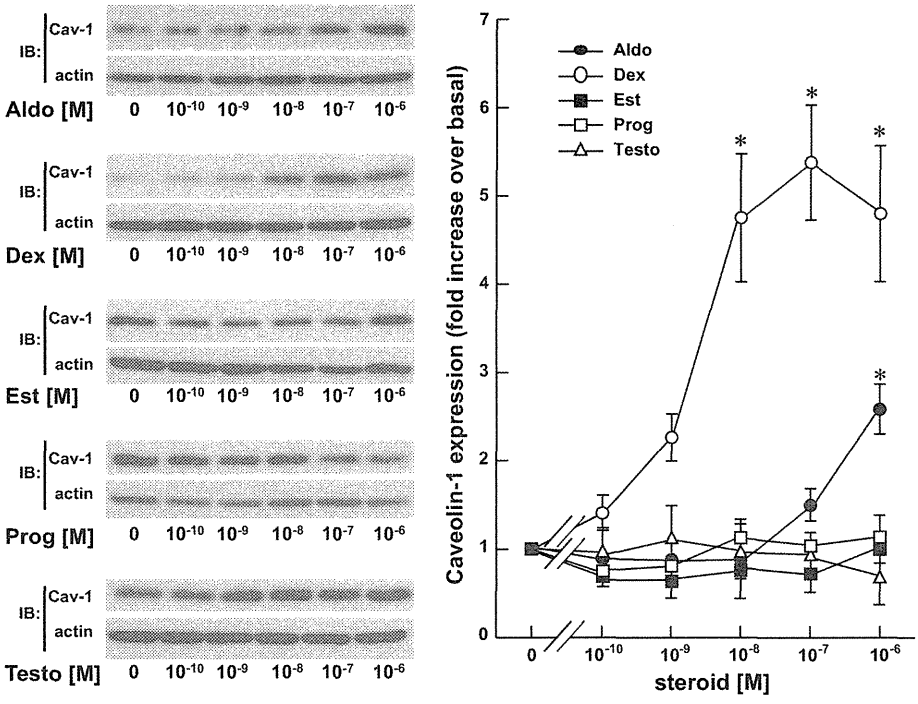

Fig. 2. Effects of various steroids on caveolin-1 protein abundance in BAEC. Shown are the results of immunoblot assays using lysates derived from BAEC treated with various steroid hormones (Aldo, aldosterone; Dex, dexamethasone; Est. 17β-estradiol; Prog, progesterone; Testo, testosterone; at the indicated concentrations for 48 h, respectively; IB, immunoblot). Cellular proteins were probed with antibodies directed to Cav-1 and actin. *Left*: data are representative of 4 independent experiments that yielded equivalent results. *Right*: results of densitometric analyses from pooled data, plotting the fold increase of the degree of expression levels of caveolin-1 at the indicated time point, relative to the signals obtained in the absence of steroids. *$P < 0.05$ vs. cells treated with vehicle alone.

(Fig. 3*A*). Thus caveolin-1 seems to be targeted to caveolae-like fractions even in the presence of dexamethasone after undergoing similar post-transcriptional modifications with vehicle-treated cells. We then performed a time-course assay in which BAEC were treated with 1 μM of dexamethasone for various time points, followed by immunoblot analyses. Results indicate that dexamethasone led to time-dependent increases in caveolin-1 protein abundance (Fig. 3*B*). Expression levels of several other endothelial proteins, including actin, VEGFR2, eNOS, protein kinases ERK1/2 as well as Akt, a small G-protein Rac1, did not change over these dexamethasone treatment protocols (see Figs. 3*B*, 4, and 5). We tested whether or not RU-486, a GR antagonist, and spironolactone, a MR inhibitor, counteracts steroids-induced upregulation of caveolin-1 protein in BAEC. Dexamethasone and aldosterone at 1 μM increased the abundance of caveolin-1 to the similar degrees as we observed in Fig. 2; however, promotion of caveolin-1 expression was not seen in the presence of RU-486 and spironolactone, respectively (Fig. 4, *A* and *B*). Collectively, these results serve to demonstrate that agonists for GR and MR, but not those for sex steroid receptors, are capable of upregulating the expression of caveolin-1 at the levels of protein and mRNA in BAEC.

Caveolin-1 is a key scaffolding protein of caveolae microdomains that modulates amplitudes of endothelial cell responses to various extracellular stimuli, including polypeptide growth factors such as VEGF (19). We therefore explored functional consequences of steroid induction of caveolin-1. We examined various responses of BAEC to VEGF that had been treated with or without dexamethasone for 48 h. We first examined the protein phosphorylation responses. As shown in Fig. 5*A*, the degrees of VEGF-promoted protein phosphorylation in VEGFR2 (Tyr1175), kinases Akt (Ser473), ERK1/2 (Thr202/Tyr204), and eNOS (Ser1179) were markedly attenuated in cells pretreated with dexamethasone that expressed higher amounts of caveolin-1 protein. When dexamethasone-elicited induction of caveolin-1 protein had been pharmacologically counteracted by RU-486, attenuation of these phosphorylation responses to VEGF was reversed (Fig. 5*B*). We also took genetic knockdown approach using previously established siRNA specific to bovine caveolin-1 (12) in combination with dexamethasone. When upregulation of caveolin-1 protein by dexamethasone was abrogated by siRNA transfection, attenuation of phosphorylation responses in VEGFR2, Akt ERK1/2, and eNOS proteins were completely recovered (Fig. 5*C*), although neither treatment with dexamethasone nor transfection with caveolin-1 siRNA affected abundance of total VEGFR2, Akt ERK1/2, or eNOS. Thus ability of dexamethasone to attenuate VEGF-elicited protein phosphorylation responses derives from upregulation of caveolin-1. Rac1 is a small G-protein that plays a pivotal role in mediating VEGF signaling pathways (11). Figure 6*A* indicates that Rac1 activation by VEGF was reduced in dexamethasone-pretreated cells compared with vehicle. eNOS is a downstream effector that is activated by VEGF under the control of upstream protein kinases and small G proteins (21). Figure 6*B* shows that stimulation with VEGF led to higher levels of nitric oxide production and that pretreatment with dexamethasone markedly abrogated it. When induction of caveolin-1 by dexamethasone was inhibited by siRNA transfection, attenuation of VEGF-elicited nitric oxide production was markedly counteracted (Fig. 6*C*). These data indicate that dexamethasone, which elevates caveolin-1 abundance, attenuates VEGF-activated signal transduction pathways at multiple levels including protein phosphorylation, Rac1 activation, as well as eNOS activation.

Migration and tube formation of endothelial cells in response to VEGF represent important physiological steps

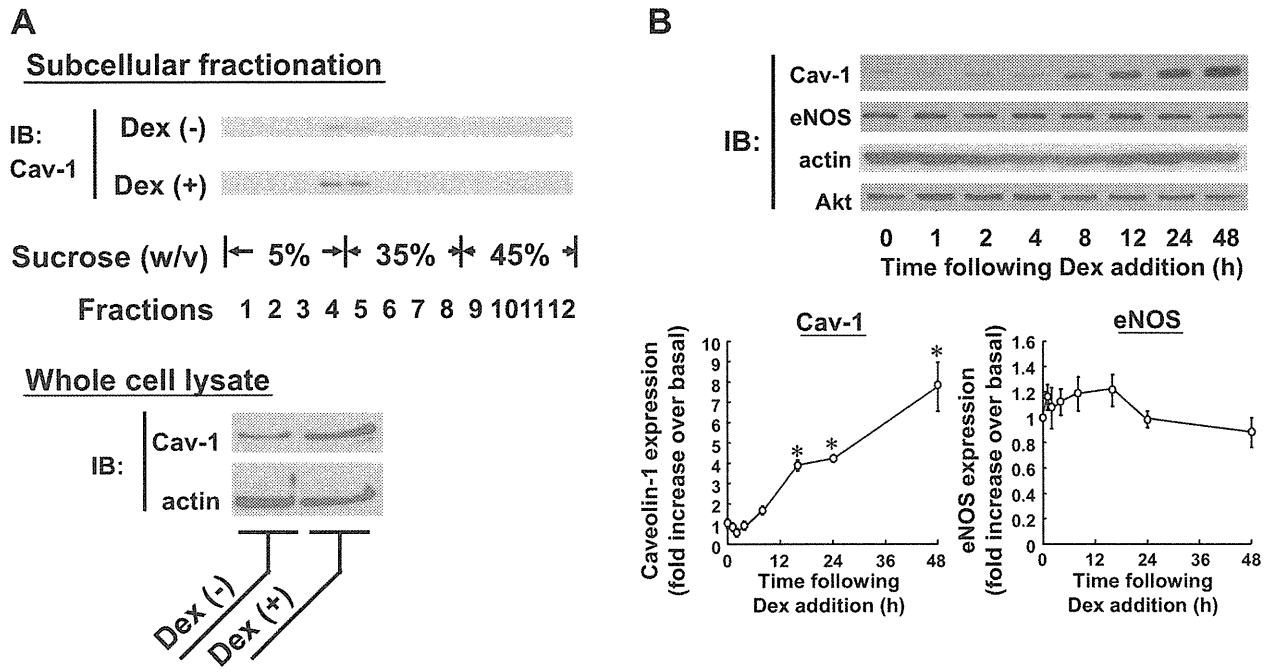

Fig. 3. Characterization of dexamethasone-induced upregulation of caveolin-1 protein abundance in BAEC. *A*: results of subcellular fractionation assay of BAEC treated with or without Dex (at 1 μM for 48 h). Sonicated cell lysates from BAEC were separated using a discontinuous sucrose gradient system as described in MATERIALS AND METHODS. An equal volume from each fraction was separated by SDS-PAGE, followed by immunoblot analysis using an antibody directed against caveolin, as indicated at *top*. An aliquot of whole cell lysate had been withdrawn before subcellular fractionation and was separately subjected to immunoblots as shown at *bottom*. Shown are representative of 3 independent experiments that yielded equivalent data. Note that Cav-1 protein in both vehicle- and Dex-treated BAEC was specifically recovered at the interface between the 5% and 35% sucrose gradient, representing the caveolae-enriched fractions. *B*: results of time course assay in which BAEC were treated with 1 μM of Dex for the indicated durations. Cellular proteins were probed with antibodies directed to Cav-1, endothelial nitric oxide synthase (eNOS), actin, and Akt. *Top*: data are representative of 4 independent experiments that yielded equivalent results. *Bottom*: results of densitometric analyses from pooled data, plotting the fold increase of the degree of expression levels of Cav-1 and eNOS at the indicated time point, relative to the signals obtained in the absence of dexamethasone. $*P < 0.05$ vs. cells treated with vehicle alone.

during angiogenic processes evoked by the growth factor (29). Using a modified Boyden chamber assay, we found that BAEC preexposed to dexamethasone exhibited lower magnitudes of migration both toward VEGF and toward serum (Fig. 7, *A* and *B*). We sought to explore the effects of dexamethasone in a human-derived endothelial cell culture model, HUVEC. Dexamethasone led to time-dependent augmentation of caveolin-1 protein abundance in HUVEC monoculture (Fig. 7*C*). Unlike in BAEC, dexamethasone attenuated eNOS protein expression. After confirming that dexamethasone induces caveolin-1 in HUVEC, we explored the effects of dexamethasone in tube forming activity using a commercially available and previously established coculture system of HUVEC with normal human fibroblasts (36). In this system, cells were incubated for 10 days in the presence and absence of dexamethasone. The degrees of endothelial tube formation were determined by means of immunostaining using an anti-CD31 antibody. Figure 7*D* indicates that the magnitude of tube formation by HUVEC in the presence of dexamethasone markedly decreased to approximately half of that seen with the vehicle. Together, these results demonstrate that endothelial cells pretreated with dexamethasone that express higher amounts of caveolin-1 exhibit attenuated responses to VEGF not only at the level of signal transduction but also at more distal levels of motility, i.e., migration and tube formation.

To explore whether or not steroids are able to upregulate caveolin-1 protein expression in vascular endothelium of living animals, we isolated thoracic aorta and lung tissues from normal male rats treated with or without dexamethasone and double-stained them with anti-caveolin-1 and anti-vWF antibodies. Caveolin-1 distributed in aorta and lung arterial cells (Fig. 8). When dexamethasone was applied for 2 days, enhanced expression of caveolin-1 was observed. Quantitative microscopic analyses revealed that endothelial caveolin-1 immunoreactive signals significantly increased by 63 ± 29% in thoracic aorta ($P < 0.05$ vs. vehicle) and tended to increase by 62 ± 13% in lung artery ($P < 0.1$). In contrast, expression of vWF of endothelial cells did not change at before and after dexamethasone treatment. These data indicate that the expression of caveolin-1 is upregulated at both aorta and lung arterial endothelial cells after dexamethasone treatment in living animals as well as in cultured endothelial cells. When whole tissue extracts were analyzed for caveolin-1 mRNA (lung and aorta, conventional RT-PCR) and protein (lung, immunoblot), we did not observe differences between dexamethasone- vs. vehicle-treated animals (data no shown). These results suggest that caveolin-1 induction by dexamethasone under these stimulation protocols occurred specifically in vascular endothelium, rather than taking place in the bulk of cell types.

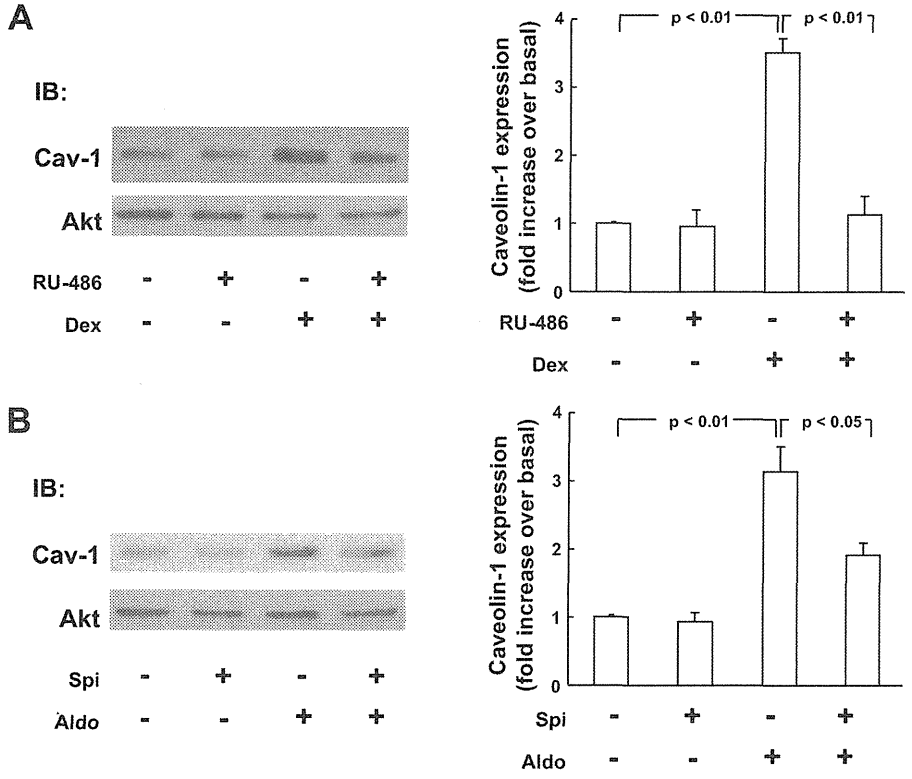

Fig. 4. Effects of steroid receptor antagonists on caveolin-1 upregulation induced by dexamethasone and aldosterone. *A*: results of protein immunoblot analyses in which effects of RU-486, a glucocorticoid receptor (GR) inhibitor, on Dex-mediated upregulation of endothelial Cav-1 protein abundance were examined. BAEC had been treated with RU-486 (1 μM for 30 min) or vehicle; an aliquot of Dex stock solution (or vehicle) was then added to the cultures to achieve a final concentration of 1 μM, as indicated. Incubation proceeded further for 48 h and protein samples were harvested and subjected to immunoblot analyses as above. *Left*: representative images. *Right*: results of densitometric analyses from pooled data, plotting the fold increase of the degree of expression levels of Cav-1, relative to the signals obtained in the absence of Dex and RU-486. *B*: spironolactone (Spi), a mineralocorticoid receptor inhibitor, and Aldo (both at 1 μM) were employed instead of RU-486 and Dex; $n = 4$ in *A* and *B*.

DISCUSSION

These results have demonstrated, for the first time to our knowledge, that the expression levels of caveolin-1 mRNA and protein in vascular endothelial cells are subjected to dynamic regulation by treatment with steroid agonists for GR and MR, associated with attenuated responses to VEGF. Induction of caveolin-1 by dexamethasone was observed in the endothelial cells derived from three independent experimental models, BAEC, HUVEC, as well as blood vessel preparations isolated from normal male rats. Furthermore, these responses took place within pharmacologically relevant drug concentrations, suggesting that caveolin-1 can be induced by steroids in multiple types of vascular endothelial cells in various experimental settings. RU-486 and spironolactone are capable of counteracting caveolin-1 induction by dexamethasone and by aldosterone, while three other sex steroids tested are without effect. Thus the abilities of steroids to augment caveolin-1 expression seem to be limited to GR and MR, but not sex steroid receptor, agonists. Caveolin-1 is known to be rather down-regulated in vascular endothelial cells by several other extracellular stimuli including cytokines and pharmacological agents (8, 15, 23). Although a glucocorticoid receptor element-like sequence has been identified at ~1,526-bp upstream of mouse caveolin-1 gene (37), the functions of these genomic elements are not currently known in endothelial cells. There remains the possibility that steroids modulate caveolin-1 expression at the levels other than transcription for example by translation, posttranscription, or degradation pathways (reviewed in Ref. 7). Some sex steroids are capable of modulating caveolin-1 expression in several nonendothelial cell types, for example, in breast (31) as well as in prostate (22) cancer cells. Thus precise molecular mechanisms whereby steroids regulate caveolin-1 expression, which are beyond the scope of current studies, remain to be elucidated both in endothelial- and nonendothelial cells.

Dexamethasone upregulates caveolin-1 in rat-derived lung epithelial cell lines (2) and in pancreatic acinar cells (24). Adipocytes express dramatically higher levels of caveolin-1 when differentiated by a hormonal mixture including dexamethasone (32). Thus these earlier observations indicate that glucocorticoid-induction of caveolin-1 is not limited to vascular endothelial cells. However, our data indicate that in whole rat organ homogenates expression levels of caveolin-1 mRNA (lung and aorta) and protein (lung) do not change 48 h after dexamethasone (data not shown), suggesting that dexamethasone does not largely affect caveolin-1 abundance in nonendothelial cell types under current protocols. Notably, functional consequences of caveolin-1 upregulation by steroids have remained completely unexplored in any cell types. We therefore sought to determine if dexamethasone leads to perturbed responses of vascular endothelial cells to extracellular stimuli. We focused on VEGF because this angiogenic growth factor represents a pivotal regulator of endothelial functions (29) and because VEGF receptor signaling is modulated by caveolae microdomains and caveolins (19, 23). VEGF activates a wide array of endothelial signal transduction pathways, starting from activation/phosphorylation of cognate receptor tyrosine kinases (VEGFR2), activation/phosphorylation of downstream protein kinases including Akt and ERK1/2, activation of a key small G-protein Rac-1, as well as eNOS-dependent nitric oxide production associated with Akt-mediated phosphorylation of

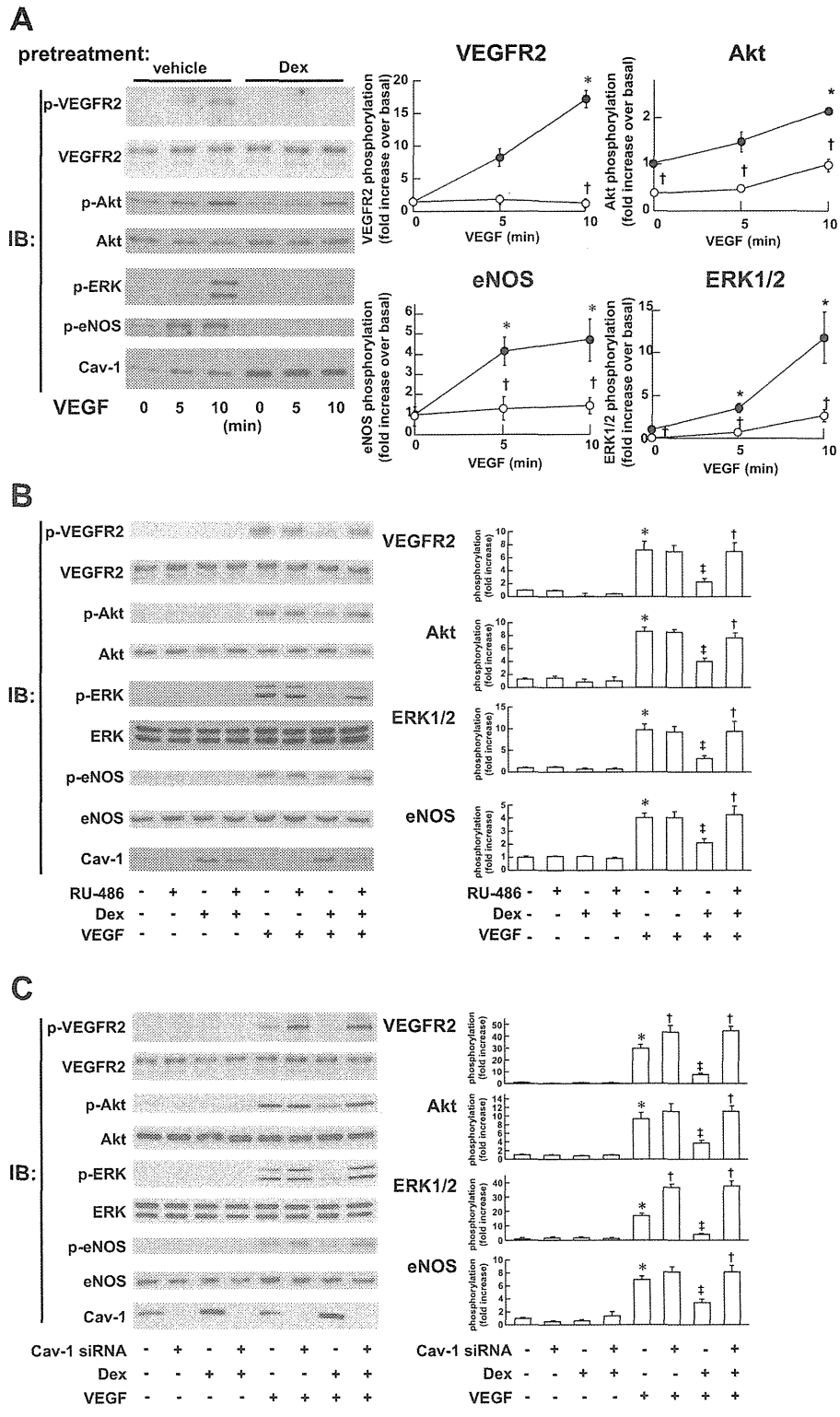

Fig. 5. Effects of dexamethasone, RU-486 and caveolin-1 specific small interfering (si)RNA on VEGF-elicited phosphorylation responses in BAEC. *A*: results of a protein immunoblot assay analyzed in cell lysates derived from BAEC treated with Dex followed by VEGF. BAEC had been incubated with Dex (1 μM for 48 h) or vehicle and then they were treated with VEGF (5 ng/ml). Following treatment with VEGF for the times indicated, cellular proteins were subjected to immunoblot assays, probed with antibodies directed to phospho-VEGFR2 (Tyr 1175), phospho-Akt (Ser473), phospho-eNOS (Ser1179), phospho-ERK1/2 (Tyr202/Thr204), and Cav-1. Equal loading of samples was confirmed by reprobing the immunoblots with antibodies against (total) VEGFR2 and Akt. *Left:* representative images. *Right:* results of densitometric analyses from pooled data, plotting the fold increase of the degree of phospho-proteins normalized to the values obtained in the absence of VEGF and Dex. Open and closed circles represent values obtained with and without pretreatment with Dex, respectively. $*P < 0.05$ vs. VEGF (−). †$P < 0.05$ vs. Dex (−); $n = 4$. *B*: cells had been pretreated with RU-486 and/or Dex (as in Fig 4*A*), followed by VEGF (5 ng/ml for 10 min). After the addition of VEGF, cells were harvested and subjected to immunoblot assays, using antibodies directed to phospho (or total)-VEGFR2, phospho (or total)-Akt, phospho (or total)-eNOS, phospho (or total)-ERK1/2, and (total) Cav-1. Pooled data of densitometry are presented in the right half, normalizing the values to those obtained in the absence of RU486, Dex and VEGF. $*P < 0.05$ vs. VEGF (−). †$P < 0.05$ vs. RU486 (−). ‡$P < 0.05$ vs. Dex (−); $n = 4$. *C*: BAEC were transfected with either control siRNA [indicated as Cav-1 siRNA (−)] or that directed to caveolin-1 [Cav-1 siRNA (+)] before dexamethasone (1 μM for 48 h) followed by VEGF (5 ng/ml for 5 min). Cells were then subjected to immunoblot analyses and densitometry as above, normalizing the values to those obtained in the absence of Dex and VEGF in control siRNA-treated cells. $*P < 0.05$ vs. VEGF (−). †$P < 0.05$ vs. control siRNA. ‡$P < 0.05$ vs. Dex (−).

eNOS protein. Our results show that when endothelial cells express higher amounts of caveolin-1 protein due to dexamethasone, these signaling events are alike attenuated. In these experiments we focused on one micromolar of dexamethasone, which has been frequently used in various cells cultures (5, 39), so as to ensure maximum caveolin-1 induction and inhibition on VEGF responses. Conversely, RU-486, a pharmacological GR antagonist, as well as transient transfection with caveolin-

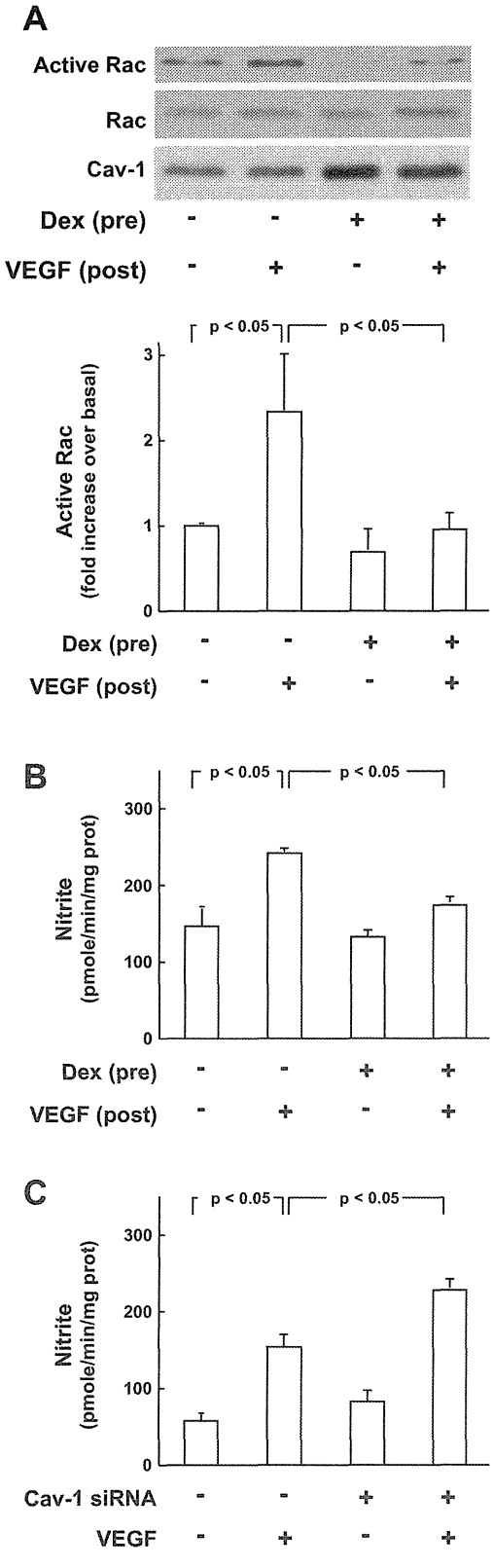

1-specific siRNA, counteracts attenuation of protein phosphorylation responses to VEGF induced by dexamethasone, concomitantly with decreases in caveolin-1. Caveolin-1 protein is supposed to be specifically targeted to plasmalemmal caveolae after completing its oligomerization processes (7). Our subcellular fractionation assays revealed that the caveolin-1 protein in BAEC is specifically targeted to caveolae-enriched fractions regardless of dexamethasone treatment. Thus the steroid agent appears to alter VEGF responses primarily by augmenting the abundance of caveolin-1 protein rather than by influencing its subcellular location and/or oligomerization status. An earlier report shows that in heterologous expression systems of 293T human fibroblast cell line, caveolin-1 acts as a direct negative regulator of VEGFR2 tyrosine kinase (19). Caveolin-1 also plays inhibitory roles in VEGF signal transduction pathways at the level of eNOS enzyme (27) and at that of upstream Rac1-Akt signaling axis (11, 12, 21). Endothelial-specific overexpression of caveolin-1 leads to impaired vascular permeability and angiogenic responses to VEGF in mice (3). When taken together with these earlier observations, the present results are consistent with a hypothesis that it is the abundance of caveolin-1 protein that plays a major role to determine the amplitudes of endothelial signaling responses to VEGF, under the control of nuclear steroid receptors. In a broader perspective, however, the roles of caveolin-1 in modulating the cellular signal transduction pathways appear to be highly complex and context dependent. For example, a stable knockdown of caveolin-1 in NIH-3T3 cells leads to augmented ERK1/2 activation (9). In contrast, in cultured endothelial cells derived from caveolin-1 null mice, VEGF-induced ERK1/2 phosphorylation responses are abrogated, rather than hyperactivated (34). Although our results are in line with the former example, these earlier studies suggest that one needs a caution in extrapolating the findings obtained in a given cellular system to the other in terms of caveolin-1 actions on receptor signal transduction pathways.

We have tested the effects of dexamethasone on migration as well as tube formation, both representing key angiogenic processes of vascular endothelial cells. Modified Boyden chamber assay revealed that cells pretreated with dexamethasone that express more abundant caveolin-1 protein display significantly lower degrees of migratory responses evoked both by VEGF and by 10% FBS in BAEC, suggesting that upregulation of caveolin-1 by dexamethasone is associated with perturbed migration toward VEGF and also likely toward some other migratory response-related bioactive substances included in the FBS. By using a previously

Fig. 6. Effects of dexamethasone on VEGF-elicited Rac1 activation and nitric oxide production in BAEC. *A*: results of Rac1 activity assay. BAEC had been incubated with Dex (1 μM for 48 h) or vehicle, then they were treated with VEGF (10 ng/ml for 1 min). Rac activity in the cell lysate was measured by means of pull-down of GTP-bound Rac1. Precipitated Rac1 was quantified in immunoblots probed with a specific monoclonal antibody. Aliquots of total cell lysates were subjected to immunoblots in separate gels using antibodies specific to Rac1 and Cav-1, as indicated; $n = 3$. *B* and *C*: results of nitrite measurement. *B*: BAEC were treated with VEGF (10 ng/ml for 6 min); some cells had been pretreated with Dex (1 μM for 48 h). Culture media were then collected and subjected to nitrite measurement as described in the text; $n = 4$. *C*: BAEC had been transfected with either control or Cav-1 specific siRNA, indicated as Cav-1 siRNA (−) or (+), respectively, before being treated with VEGF. $n = 5$.

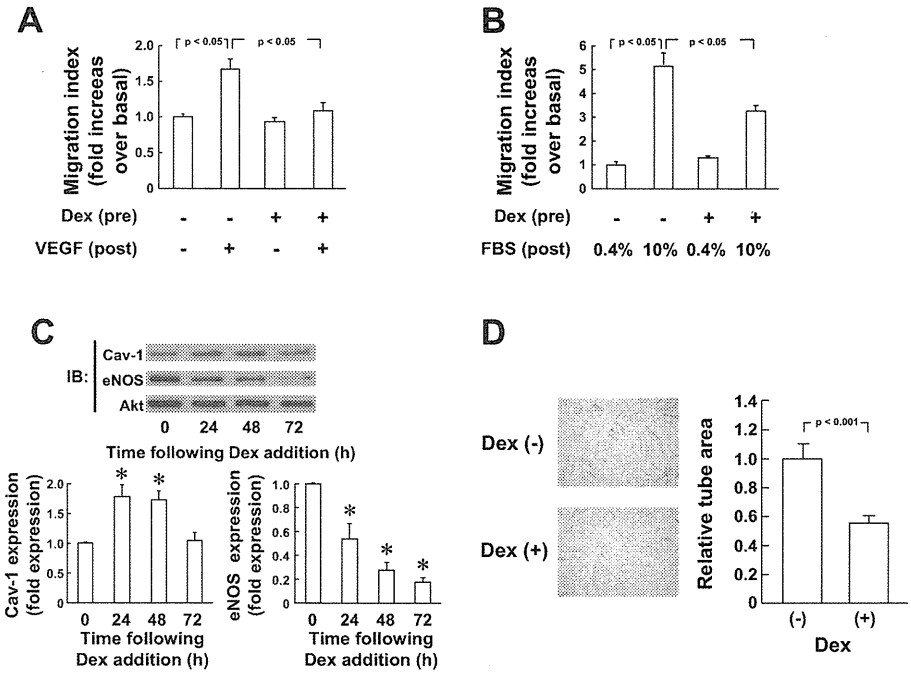

Fig. 7. Effects of dexamethasone on migratory responses in BAEC and caveolin-1 expression and tube formation activity in human umbilical vein endothelial cells (HUVEC). *A* and *B*: results of cell migration assay. BAEC had been pretreated with Dex (1 μM) or vehicle for 48 h. Then, they were trypsinized and applied for cell migration assay as described in the text. Cells were stimulated with 10 ng/ml of VEGF for 6 h (*A*) or different concentrations of FBS for 4 h (*B*) in the outer chamber during migration assay. The degrees of cell migration across the filter membranes were assessed as optical density at 560 nm, normalized to the values obtained in the absence of Dex and VEGF (*A*) or in the presence of 0.4% FBS alone (*B*), and expressed as fold increase over basal (migration index); $n = 3$, respectively. *C*: immunoblot analyses were performed in HUVEC monoculture that had been treated with Dex. Cells were treated with Dex (1 μM) for the times indicated. *Top*: representative immunoblots probed using antibodies as illustrated. *Bottom*: graphs show the results of densitometric analyses from pooled data, plotting the fold increases in expression levels of caveolin-1 and eNOS at the indicated Dex treatment duration, relative to the signals obtained in the absence of Dex; $n = 6$. $^*P < 0.05$ vs. cells not treated with dexamethasone. *D*: tube formation assay was performed using a coculture system of HUVEC and normal human fibroblasts. Endothelial cells were identified using an CD-31 antibody 10 days after the incubation with Dex (10 μM) or vehicle. *Left*: typical microphotogram depicting attenuated tube formation in the presence of dexamethasone (*bottom*) compared with vehicle (*top*). Tube area was estimated from 4 pictures from each well and the area of the formed tube was represented as a relative value to that formed in the wells with vehicle control. Pooled results obtained from 6 independent experiments are summarized at *right*.

established coculture model of HUVEC with normal human fibroblasts, we showed that incubation of these cells with dexamethasone for 10 days leads to attenuated endothelial tube formation activity, identified with an anti-CD31 antibody. Our earlier experiments suggested that VEGF receptor ligands endogenously secreted by adjacent fibroblasts in coculture play a significant role to promote tube formation of HUVEC in this system (36). When taken together with the fact that dexamethasone is capable of increasing caveolin-1 abundance in HUVEC monoculture, reaching to the maximum level 2 days after drug addition, our data support a hypothesis that attenuation of tube formation in HUVEC by dexamethasone occurs due to increases in caveolin-1 abundance that affects VEGF pathways. We cannot rule out the possibility that the regulatory pattern of caveolin-1 abundance in dexamethasone-treated HUVEC in coculture exhibits somewhat different kinetics compared with those actually examined in monoculture in this study, although we added fresh dexamethasone every 3 days during the tube formation assay. Plausibly, steroids, especially corticosteroids, are associated with attenuated degrees of VEGF-induced angiogenic responses in humans (13) and in experimental animal models (16, 25). Serum VEGF levels are elevated in patients with Cushing's syndrome when compared with those suffer from essential hypertension (18), suggesting some functional linkages of VEGF and steroid pathways in humans. We propose that regulation of caveolin-1 abundance by nuclear steroid receptor pathways may uncover a novel mechanism at which exposure to excess steroids, including agonists for GR and MR, leads to perturbed sensitivities of vascular endothelium to angiogenic growth factors such as VEGF. Although our experiments using normal male rats demonstrate that administration with a GR agonist can upregulate caveolin-1 in living animals, it remains to be seen if this were the case with human subjects.

In these experimental settings, expression levels of several other proteins including actin, VEGFR2, Akt, ERK1/2, and Rac1 did not change over various stimulation protocols with steroid receptor agonists, suggesting that steroid induction of endothelial caveolae-related proteins is relatively specific to caveolin-1. In some immunoblot assays we exploited Akt as a loading control because in these panels we performed phospho-Western analyses of this protein, because steroids did not alter its expression, and because the anti-Akt antibody used in this study yielded relatively strong and specific immunoreactive signals in our system. As to eNOS, dexamethasone leads to significant down-regulation of its protein expression level in HUVEC, although it does not do so in BAEC. This implies that

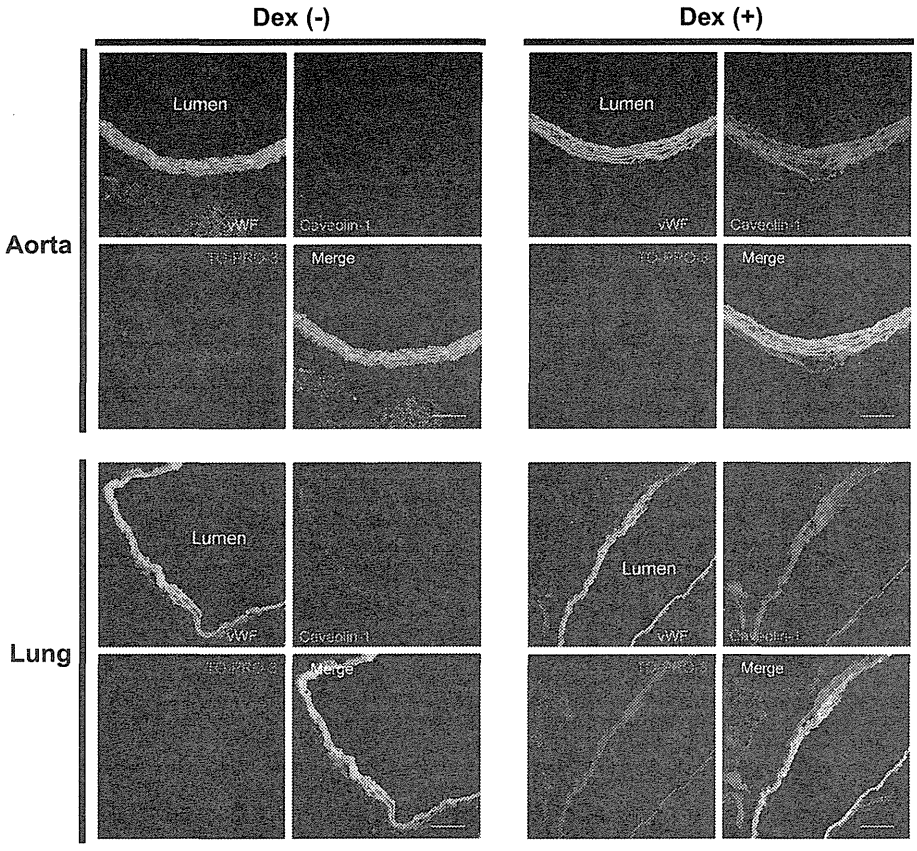

Fig. 8. Effects of dexamethasone on caveolin-1 expression in rat aortic endothelium. Shown are the representative double staining experiments with anti-von Willebrand factor (vWF) antibody (green fluorescence) and anti-caveolin-1 antibody (red fluorescence) of thoracic aorta and lung arterial cells. TO-PRO-3 was used for nuclear detection (blue fluorescence). Forty-eight hours after intraperitoneal injection of dexamethasone (0.1 mg kg/body wt), upregulation of caveolin-1 expression was observed in aorta and lung arterial cells. Scale bars = 100 μm; n = 6.

regulation of eNOS expression levels by steroids takes place on an endothelial cell subtype-specific fashion. Nonetheless, BAEC preexposed to dexamethasone exert attenuated levels of VEGF-stimulated nitric oxide production compared with vehicle control cells, despite total eNOS protein expression levels being constant. Earlier studies provided several other mechanisms whereby steroids may lead to dysfunction of eNOS system. These include down-regulation of eNOS mRNA/protein (38, 39), tetrahydrobiopterin insufficiency leading to eNOS "uncoupling" (28), or down-regulation of glucose-6-phosphate dehydrogenase activity (20). Thus our results may now identify an additional point of regulation at which these steroid receptor agonists decrease nitric oxide production even at the situation where they do not alter total eNOS abundance, provided that caveolin-1 has been established as a key inhibitory binding partner of eNOS protein (27). In our system, simple transfection with caveolin-1 specific siRNA did not increase basal NO production with a statistical significance. This may be due to the degrees of caveolin-1 protein knockdown, the sensitivity of our detection method, or some other experimental conditions.

In summary, we have demonstrated that pharmacologically relevant doses of GR and MR agonists induce caveolin-1, a major regulatory protein of plasmalemmal caveolae, in cultured vascular endothelial cells. Cells pretreated with dexamethasone that express higher levels of caveolin-1 exhibit attenuated responses to a polypeptide growth factor VEGF at the levels of signal transduction, cell migration, and tube formation. We propose that steroid-induced upregulation of caveolin-1 identifies a novel point of control at which ligands for nuclear receptors modulate signal transduction pathways activated by cell surface receptors in vascular endothelium. Because treatment with dexamethasone appears to augment caveolin-1 expression in vascular endothelium in living animals as well, our study may also provide another mechanism underlying cardiovascular disorders associated with perturbation of steroid hormone systems.

ACKNOWLEDGMENTS

We thank Toshitaka Nakagawa and Miyako Daike (Kagawa University) for superlative technical assistance.

GRANTS

This study was supported in part by a Grant-in-Aid for Scientific Research (C) to J. Igarashi (21590933) and to Y. Kubota (24591654) from the Ministry of Education, Culture, Sports, Science and Technology of Japan.

DISCLOSURES

No conflicts of interest, financial or otherwise, are declared by the author(s).

AUTHOR CONTRIBUTIONS

Author contributions: J.I. conception and design of research; J.I., T.H., K.S., K.Y., I.T., T.M., and H.K. performed experiments; J.I. and T.H. analyzed data; J.I., Y.K., and H.K. interpreted results of experiments; J.I., K.Y., and I.T. prepared figures; J.I. and K.Y. drafted manuscript; J.I. and T.H. edited and revised manuscript; J.I., T.H., K.S., K.Y., I.T., Y.K., and H.K. approved final version of manuscript.

REFERENCES

1. **Akaza I, Yoshimoto T, Tsuchiya K, Hirata Y.** Endothelial dysfunction associated with hypercortisolism is reversible in Cushing's syndrome. *Endocr J* 57: 245–252, 2010.
2. **Barar J, Campbell L, Hollins AJ, Thomas NP, Smith MW, Morris CJ, Gumbleton M.** Cell selective glucocorticoid induction of caveolin-1 and caveolae in differentiating pulmonary alveolar epithelial cell cultures. *Biochem Biophys Res Commun* 359: 360–366, 2007.
3. **Bauer PM, Yu J, Chen Y, Hickey R, Bernatchez PN, Looft-Wilson R, Huang Y, Giordano F, Stan RV, Sessa WC.** Endothelial-specific expression of caveolin-1 impairs microvascular permeability and angiogenesis. *Proc Natl Acad Sci USA* 102: 204–209, 2005.
4. **Baykan M, Erem C, Gedikli O, Hacihasanoglu A, Erdogan T, Kocak M, Durmus I, Korkmaz L, Celik S.** Impairment of flow-mediated vasodilatation of brachial artery in patients with Cushing's syndrome. *Endocrine* 31: 300–304, 2007.
5. **Brostjan C, Anrather J, Csizmadia V, Stroka D, Soares M, Bach FH, Winkler H.** Glucocorticoid-mediated repression of NFkappaB activity in endothelial cells does not involve induction of IkappaBalpha synthesis. *J Biol Chem* 271: 19612–19616, 1996.
6. **Catena C, Colussi G, Nadalini E, Chiuch A, Baroselli S, Lapenna R, Sechi LA.** Cardiovascular outcomes in patients with primary aldosteronism after treatment. *Arch Intern Med* 168: 80–85, 2008.
7. **Cohen AW, Hnasko R, Schubert W, Lisanti MP.** Role of caveolae and caveolins in health and disease. *Physiol Rev* 84: 1341–1379, 2004.
8. **Feron O, Dessy C, Desager JP, Balligand JL.** Hydroxy-methylglutaryl-coenzyme A reductase inhibition promotes endothelial nitric oxide synthase activation through a decrease in caveolin abundance. *Circulation* 103: 113–118, 2001.
9. **Galbiati F, Volonte D, Engelman JA, Watanabe G, Burk R, Pestell RG, Lisanti MP.** Targeted downregulation of caveolin-1 is sufficient to drive cell transformation and hyperactivate the p42/44 MAP kinase cascade. *EMBO J* 17: 6633–6648, 1998.
10. **Gill GN, Ill CR, Simonian MH.** Angiotensin stimulation of bovine adrenocortical cell growth. *Proc Natl Acad Sci USA* 74: 5569–5573, 1977.
11. **Gonzalez E, Kou R, Michel T.** Rac1 modulates sphingosine 1-phosphate-mediated activation of phosphoinositide 3-kinase/Akt signaling pathways in vascular endothelial cells. *J Biol Chem* 281: 3210–3216, 2006.
12. **Gonzalez E, Nagiel A, Lin AJ, Golan DE, Michel T.** Small interfering RNA-mediated down-regulation of caveolin-1 differentially modulates signaling pathways in endothelial cells. *J Biol Chem* 279: 40659–40669, 2004.
13. **Greenberger S, Boscolo E, Adini I, Mulliken JB, Bischoff J.** Corticosteroid suppression of VEGF-A in infantile hemangioma-derived stem cells. *N Engl J Med* 362: 1005–1013, 2010.
14. **Igarashi J, Miyoshi M, Hashimoto T, Kubota Y, Kosaka H.** Statins induce S1P(1) receptors and enhance endothelial nitric oxide production in response to high-density lipoproteins. *Br J Pharmacol* 150: 470–479, 2007.
15. **Igarashi J, Shoji K, Hashimoto T, Moriue T, Yoneda K, Takamura T, Yamashita T, Kubota Y, Kosaka H.** Transforming growth factor-beta1 downregulates caveolin-1 expression and enhances sphingosine 1-phosphate signaling in cultured vascular endothelial cells. *Am J Physiol Cell Physiol* 297: C1263–C1274, 2009.
16. **Kasselman LJ, Kintner J, Sideris A, Pasnikowski E, Krellman JW, Shah S, Rudge JS, Yancopoulos GD, Wiegand SJ, Croll SD.** Dexamethasone treatment and ICAM-1 deficiency impair VEGF-induced angiogenesis in adult brain. *J Vasc Res* 44: 283–291, 2007.
17. **Kim KH, Moriarty K, Bender JR.** Vascular cell signaling by membrane estrogen receptors. *Steroids* 73: 864–869, 2008.
18. **Kristo C, Ueland T, Godang K, Aukrust P, Bollerslev J.** Biochemical markers for cardiovascular risk following treatment in endogenous Cushing's syndrome. *J Endocrinol Invest* 31: 400–405, 2008.
19. **Labrecque L, Royal I, Surprenant DS, Patterson C, Gingras D, Beliveau R.** Regulation of vascular endothelial growth factor receptor-2 activity by caveolin-1 and plasma membrane cholesterol. *Mol Biol Cell* 14: 334–347, 2003.
20. **Leopold JA, Dam A, Maron BA, Scribner AW, Liao R, Handy DE, Stanton RC, Pitt B, Loscalzo J.** Aldosterone impairs vascular reactivity by decreasing glucose-6-phosphate dehydrogenase activity. *Nat Med* 13: 189–197, 2007.
21. **Levine YC, Li GK, Michel T.** Agonist-modulated regulation of AMP-activated protein kinase (AMPK) in endothelial cells: evidence for an AMPK -> Rac1 -> Akt -> endothelial nitric-oxide synthase pathway. *J Biol Chem* 282: 20351–20364, 2007.
22. **Li L, Yang G, Ebara S, Satoh T, Nasu Y, Timme TL, Ren C, Wang J, Tahir SA, Thompson TC.** Caveolin-1 mediates testosterone-stimulated survival/clonal growth and promotes metastatic activities in prostate cancer cells. *Cancer Res* 61: 4386–4392, 2001.
23. **Liu J, Razani B, Tang S, Terman BI, Ware JA, Lisanti MP.** Angiogenesis activators and inhibitors differentially regulate caveolin-1 expression and caveolae formation in vascular endothelial cells. Angiogenesis inhibitors block vascular endothelial growth factor-induced down-regulation of caveolin-1. *J Biol Chem* 274: 15781–15785, 1999.
24. **Liu P, Li WP, Machleidt T, Anderson RG.** Identification of caveolin-1 in lipoprotein particles secreted by exocrine cells. *Nat Cell Biol* 1: 369–375, 1999.
25. **Luo JC, Shin VY, Liu ES, Ye YN, Wu WK, So WH, Chang FY, Cho CH.** Dexamethasone delays ulcer healing by inhibition of angiogenesis in rat stomachs. *Eur J Pharmacol* 485: 275–281, 2004.
26. **Mancini T, Kola B, Mantero F, Boscaro M, Arnaldi G.** High cardiovascular risk in patients with Cushing's syndrome according to 1999 WHO/ISH guidelines. *Clin Endocrinol (Oxf)* 61: 768–777, 2004.
27. **Michel T, Feron O.** Nitric oxide synthases: which, where, how, and why? *J Clin Invest* 100: 2146–2152, 1997.
28. **Nagata D, Takahashi M, Sawai K, Tagami T, Usui T, Shimatsu A, Hirata Y, Naruse M.** Molecular mechanism of the inhibitory effect of aldosterone on endothelial NO synthase activity. *Hypertension* 48: 165–171, 2006.
29. **Neufeld G, Cohen T, Gengrinovitch S, Poltorak Z.** Vascular endothelial growth factor (VEGF) and its receptors. *FASEB J* 13: 9–22, 1999.
30. **Patel HH, Murray F, Insel PA.** Caveolae as organizers of pharmacologically relevant signal transduction molecules. *Annu Rev Pharmacol Toxicol* 48: 359–391, 2008.
31. **Salatino M, Beguelin W, Peters MG, Carnevale R, Proietti CJ, Galigniana MD, Vedoy CG, Schillaci R, Charreau EH, Sogayar MC, Elizalde PV.** Progestin-induced caveolin-1 expression mediates breast cancer cell proliferation. *Oncogene* 25: 7723–7739, 2006.
32. **Scherer PE, Lisanti MP, Baldini G, Sargiacomo M, Mastick CC, Lodish HF.** Induction of caveolin during adipogenesis and association of GLUT4 with caveolin-rich vesicles. *J Cell Biol* 127: 1233–1243, 1994.
33. **Song KS, Li S, Okamoto T, Quilliam LA, Sargiacomo M, Lisanti MP.** Co-purification and direct interaction of Ras with caveolin, an integral membrane protein of caveolae microdomains. Detergent-free purification of caveolae microdomains. *J Biol Chem* 271: 9690–9697, 1996.
34. **Sonveaux P, Martinive P, DeWever J, Batova Z, Daneau G, Pelat M, Ghisdal P, Gregoire V, Dessy C, Balligand JL, Feron O.** Caveolin-1 expression is critical for vascular endothelial growth factor-induced ischemic hindlimb collateralization and nitric oxide-mediated angiogenesis. *Circ Res* 95: 154–161, 2004.
35. **Tauchmanova L, Rossi R, Biondi B, Pulcrano M, Nuzzo V, Palmieri EA, Fazio S, Lombardi G.** Patients with subclinical Cushing's syndrome due to adrenal adenoma have increased cardiovascular risk. *J Clin Endocrinol Metab* 87: 4872–4878, 2002.
36. **Tsukamoto I, Sakakibara N, Maruyama T, Igarashi J, Kosaka H, Kubota Y, Tokuda M, Ashino H, Hattori K, Tanaka S, Kawata M, Konishi R.** A novel nucleic acid analogue shows strong angiogenic activity. *Biochem Biophys Res Commun* 399: 699–704, 2010.
37. **van Batenburg MF, Li H, Polman JA, Lachize S, Datson NA, Bussemaker HJ, Meijer OC.** Paired hormone response elements predict caveolin-1 as a glucocorticoid target gene. *PLos One* 5: e8839, 2010.
38. **Wallerath T, Godecke A, Molojavyi A, Li H, Schrader J, Forstermann U.** Dexamethasone lacks effect on blood pressure in mice with a disrupted endothelial NO synthase gene. *Nitric Oxide* 10: 36–41, 2004.
39. **Wallerath T, Witte K, Schafer SC, Schwarz PM, Prellwitz W, Wohlfart P, Kleinert H, Lehr HA, Lemmer B, Forstermann U.** Down-regulation of the expression of endothelial NO synthase is likely to contribute to glucocorticoid-mediated hypertension. *Proc Natl Acad Sci USA* 96: 13357–13362, 1999.
40. **Walters EH, Reid D, Soltani A, Ward C.** Angiogenesis: a potentially critical part of remodelling in chronic airway diseases? *Pharmacol Ther* 118: 128–137, 2008.
41. **Yoneda K, Fujimoto T, Imamura S, Ogawa K.** Distribution of fodrin in the keratinocyte in vivo and in vitro. *J Invest Dermatol* 94: 724–729, 1990.

Experimental dermatology • **Original article**

CED
Clinical and Experimental Dermatology

Sphingosine 1-phosphate attenuates peroxide-induced apoptosis in HaCaT cells cultured *in vitro*

T. Moriue,[1] J. Igarashi,[2] K. Yoneda,[1] T. Hashimoto,[2] K. Nakai,[2] H. Kosaka[2] and Y. Kubota[1]

Departments of [1]Dermatology and [2]Cardiovascular Physiology, Faculty of Medicine, Kagawa University, Kagawa, Japan

doi:10.1111/ced.12037

Summary

Background. Sphingosine 1-phosphate (S1P) is a sphingolipid mediator that elicits a wide array of physiological responses in various types of mammalian cells. Among the numerous biological activities elicited by S1P is protection from apoptotic cell death, which seems to take place through the cell-surface S1P receptor and the downstream phosphoinositide 3′-OH kinase (PI3-K)/Akt pathway. It is unclear whether and how S1P protects human keratinocytes from hydrogen peroxide (H_2O_2)-induced apoptosis.

Aim. We investigated the effects of S1P on apoptotic cell death in HaCaT cells, spontaneously immortalized human keratinocytes.

Methods. HaCaT cells were treated with hydrogen peroxide (H_2O_2) 1–2 mmol/L as an inducer of apoptosis. Cellular apoptosis was assessed with terminal dUTP nick-end labelling (TUNEL), WST-8 and immunoblot assays.

Results. In WST-8 and TUNEL assays, S1P pretreatment (1 μmol/L for 30 min) attenuated H_2O_2-induced cell death. Promotion of the cleavage of caspase-3 by H_2O_2 was markedly attenuated when cells had been preincubated with S1P. S1P markedly potentiated phosphorylation (activation) of Akt in the presence of H_2O_2. Wortmannin, a selective inhibitor of the PI3-K/Akt pathway, significantly suppressed S1P-induced attenuation of caspase-3 cleavage promoted by H_2O_2.

Conclusions. S1P, a sphingolipid mediator, attenuates H_2O_2-induced apoptosis of HaCaT cells, by promoting phosphorylation of the Akt pathway.

Introduction

Sphingosine 1-phosphate (S1P) is a sphingolipid mediator that elicits a wide variety of biological actions in numerous mammalian cell types.[1] Specifically in keratinocytes, S1P evokes such important responses as proliferation,[2] differentiation[2,3] and migration.[4] An antiapoptotic effect represents another important function of S1P. In keratinocytes, S1P attenuates apoptotic cell death induced by actinomycin, tumour necrosis factor (TNF)-α,[5] ceramide[6] and ultraviolet (UV)B irradiation.[7]

It is known that skin wounding causes oxidative stress, defined as excess production of reactive oxygen species (ROS). For example, increased levels of hydrogen peroxide (H_2O_2) are detected in wound fluid.[8] Oxidative stress may function as a 'double-edged sword' in the wound-healing process, as it promotes coagulation, initiation of inflammation, re-epithelization, angiogenesis and matrix deposition, while inhibiting migration and inducing apoptosis in keratinocytes.[9] It is therefore important to better elucidate the effects of ROS on keratinocytes and how bioactive substances modulate such processes.

Recently, we reported that S1P attenuates H_2O_2-induced apoptosis of cultured vascular endothelial cells, associated with attenuation of p38 MAP kinase

Correspondence: Dr Tetsuya Moriue, Department of Dermatology, Faculty of Medicine, Kagawa University, 1750-1 Ikenobe, Miki-Cho, Kita-Gun, Kagawa 761-0793, Japan
E-mail: moririn@med.kagawa-u.ac.jp

Conflict of interest: none declared.

Accepted for publication 22 July 2012

activation.[10] However, it remains unclear whether and how S1P protects human keratinocytes from H_2O_2-induced apoptosis.[11] In the present study, we investigated the effects of S1P on apoptotic cell death in HaCaT cells, spontaneously immortalized human keratinocytes.

Methods

Cell culture and drug treatments

HaCaT cells[12,13] were split at a ratio of 1 : 4 and maintained in DMEM (Sigma Chemical Co., St. Louis, MO, USA), supplemented with heat-inactivated fetal bovine serum (FBS; 10%, v/v) and streptomycin (100 U/mL and 100 mg/mL) on culture plates. They were kept at 37 °C in a humidified atmosphere containing 5% CO_2. At 70–80% confluence, the culture medium was changed to DMEM without FBS, and the cells incubated for 30 min before any further experiments to exclude the effects of any residual S1P contained in the FBS.

WST-8 assay of cell viability

HaCaT cell viability was assessed using a 2-(2-methoxy-4-nitrophenyl)-3-(4-nitrophenyl)-5-(2,4-disulfophenyl)-2H-tetrazolium (WST-8) assay, in accordance with the manufacturer's instructions. Briefly, cells were split at a ratio of 1 : 8 and were transferred to a 96-well plate, then mixed with 10 μl of CCK-8 solution from a commercial kit (Dojindo, Tokyo, Japan).and incubated for 1 h at 37 °C in a CO_2 incubator. Some cells were pretreated with 1 μmol/L S1P for 30 min, and all cells (pretreated or not) were then treated with 750 μmol/L H_2O_2 or vehicle for 4 h. After treatment, cells were mixed with 10 μL of CCK-8 solution from a commercial kit (Dojindo, Tokyo, Japan), and incubated for 1 h at 37 °C in a CO_2 incubator. Cell viability was determined by measuring optical density (OD) at 450 nm using a microplate reader (model SH-9000; Hitachi Hi-Technologies, Tokyo, Japan) In each experiment, the OD 450 nm values were normalized to those with H_2O_2 alone, which yielded minimum values within each experiment.

Terminal dUTP nick-end labelling assay

The degrees of DNA nick formation were determined *in situ* by a terminal dUTP nick-end labelling (TUNEL) assay. HaCaT cells were split at a ratio of 1 : 24 and seeded onto coverslips. At approximately 30% confluence, 4 days after being split, the cells were starved of serum. They were washed with phosphate-buffered saline (PBS) on ice, and fixed with 1% paraformaldehyde in PBS (w/v) for 10 min at ambient temperature, followed by permeabilization with acetone/ethanol (1 : 2 v/v) for 5 min at −20 °C. The TUNEL assay was then performed with a commercial kit (ApopTag Fluorescein *In Situ* Apoptosis Detection Kit; Chemicon, Temecula, CA, USA) in accordance with the the manufacturer's instructions. To determine the number of TUNEL-positive cells, 1000 cells were counted using fluorescent microscopy, with five independent microscopic fields counted in each coverslip at ×40 magnification. The percentage of TUNEL-positive cells was calculated as:

(total number of TUNEL-positive cells ÷ total number of all cells) × 100.

Immunoblotting analyses

HaCaT cells were split at a ratio of 1 : 4, and cultured on plastic dishes. Immunoblotting analyses were performed as described previously.[14] Briefly, the membrane was probed with an antibody against the cleaved form of caspase-3 (Asp^{175}) protein (Cell Signaling Technology Inc., Beverly, MA, USA). Equal amounts of protein (50 μg) were loaded per lane. Blots were re-probed with an antibody directed to (total) actin to confirm equal loading (not shown). Signals corresponding to the cleaved form of caspase-3 were quantified and normalized against the value obtained with H_2O_2 alone (maximum) in each experiment.

Akt analyses

HaCaT cells were divided into two groups: one group was pretreated with S1P 1 μmol/L for 30 min, then all cells were treated with H_2O_2 1 mmol/L for 0, 5, 15, 30, 45 and 60 minutes. Signals corresponding to phosphorylated forms of Akt were quantified and normalized against the values obtained using antibodies specific to total Akt (Cell Signaling Technology Inc.). Equal amounts of protein (30 μg) were loaded per lane, and the resulting ratios of phosphorylated (Ser^{473}; Cell Signaling Technology Inc.) to total Akt were then normalized to the basal value obtained in the absence of H_2O_2 and S1P.

Cells were also treated with wortmannin (Merck, Darmstadt, Germany) dissolved in 0.1% (v/v) dimethyl sulfoxide (DMSO) to examine the effect on H_2O_2-induced phosphorylation of Akt and cleavage of caspase-3. HaCaT cells were pretreated with wortmannin 10 nmol/L for 30 min, then treated with $H2O_2$ or

vehicle (distilled water) for 15 min. Equal amounts of protein (100 μg) were loaded onto protein gels and immunoblotted. Some cells were pretreated with S1P 1 μmol/L for 30 min, and the membrane was probed for the cleaved form of caspase-3 protein. Equal amounts of protein (100 μg) were loaded per lane, and blots were re-probed with an antibody directed to total actin to confirm equal loading.

Supplementary experiments

We used reverse transcription (RT)-PCR to detect transcripts encoding $S1P_1$ to $S1P_5$ (see supplementary figures for details). Actin and glyceraldehyde 3-phosphate dehydrogenase were used as housekeeping genes (Table S1).

Next, HaCaT cells were pretreated with FTY720-P1 (Cayman Chemical Co., Ann Arbor, MI, USA) 1 μmol/L for 30 min to assesses whether it enhanced H_2O_2-elicited Akt phosphorylation.

Activation of signal transducer and activator of transcription (Stat)3, which mediates the H_2O_2-elicited cellular damage, was also assessed, using phospho-Stat3 (Tyr^{705}/Ser^{727}; Cell Signaling Technology Inc.).

We also evaluated the effects of H_2O_2 and/or S1P on mitogen-activated protein kinases (MAPKs) by assessing the degrees of phosphorylation, using antibodies to phospho-p38 (Thr^{180}/Tyr^{182}), total p38, phospho-Jun kinase (JNK; Thr^{183}/Tyr^{185}), total JNK, phospho-extracellular signal-regulated kinase (ERK)1/2 (Thr^{202}/Tyr^{204}) and total ERK1/2 (all Cell Signaling Technology Inc.).

Statistical analysis

All experiments were performed at least 3 times. Mean values for individual experiments are expressed as means ± SE. Significant differences between two groups were analysed by Student's *t*-test using Microsoft Excel. $P < 0.05$ was considered significant.

Results

WST-8 assay of cell viability

The WST-8 assay showed that survival of HaCaT cells 4 h after treatment with H_2O_2 750 μmol/L was significantly ($P = 0.04$) decreased to 57.9 ± 7.4% of baseline (Fig. 1a). Importantly, when cells had been exposed to S1P before H_2O_2, attenuation of cellular viability was reversed to 82.5 ± 6.2% ($P = 0.04$).

Terminal dUTP nick-end labelling assay

A significantly larger number of TUNEL-positive nuclei (Fig. 1: green staining, arrowheads) were seen in HaCaT cells 4 h after treatment with H_2O_2 750 μmol/L compared with untreated cells, showing that their DNA was nicked upon H_2O_2 treatment. The fraction of TUNEL-positive cells increased after H_2O_2 treatment by 14-fold from basal levels ($P = 0.01$). Pretreatment with 1 μmol/L S1P decreased the fraction of TUNEL-positive cells by 21.4% ($P = 0.03$) compared with those treated with H_2O_2 alone (Fig. 1c).

Immunoblotting analyses

H_2O_2 induced cleavage (activation) of caspase-3 protein, which was markedly attenuated when cells were preincubated with S1P.

Akt analyses

The amount of phosphorylated Akt, increased slightly, but did not reach significance after treatment with H_2O_2 750 μmol/L alone (Fig. 2). However, pretreatment with S1P 1 μmol/L for 30 min significantly enhanced the H_2O_2-elicited Akt phosphorylation, and this was visible 15 min after H_2O_2 treatment.

Pretreatment with wortmannin significantly ($P = 0.001$) attenuated the degree of S1P-induced phosphorylation of Akt (Fig. 3a), and markedly increased H_2O_2-evoked cleavage of caspase-3 ($P < 0.01$). S1P was incapable of protecting HaCaT cells from the H_2O_2-elicited cleavage of caspase-3 in the presence of wortmannin (Fig. 3b).

Supplementary experiments

Using RT-PCR, transcripts encoding $S1P_1$ to $S1P_5$ were detected (Fig. S1).

Pretreatment of HaCaT cells with FTY720-P 1 μmol/L for 30 min significantly enhanced the H_2O_2-elicited Akt phosphorylation at 5 min (Fig. S2).

We explored Stat3 phosphorylation with western blot analysis. When cells were pretreated with FTY720-P, phosphorylation of Ser^{727} was attenuated ($P < 0.05$) but not that of $Tyr7^{05}$ (Fig. S3).

H_2O_2 induced a robust phosphorylation (activation) response of MAPKs. S1P did not affect the degree of phosphorylation of p38, JNK and ERK1/2 (data not shown). An increase in S1P from 1 to 10 μmol/L did not alter the degree of Akt phosphorylation in the presence of successively administered H_2O_2 (Fig S4),

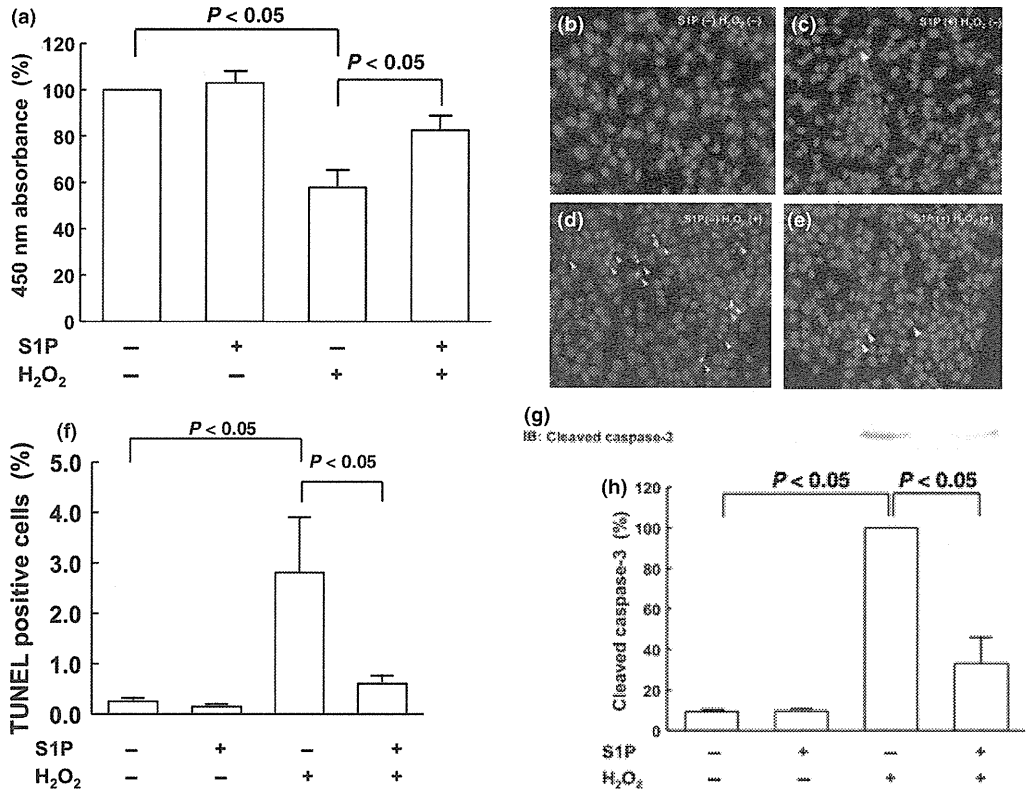

Figure 1 (a) In the WST-8 assay, sphingosine 1-phosphate (S1P) pretreatment reduced the H_2O_2-induced apoptotic responses of HaCaT cells. Each data point represents mean ± SE; n = 4. (b–e) Terminal dUTP nick-end labelling assay, using fluorescent microscopy (yellow arrowheads indicate TUNEL-positive signals). (f) Quantification of TUNEL-positive cell numbers as a percentage of the total. Each data point represents mean ± SE; n = 5. (g) Representative image of immunoblot after H_2O_2/S1P treatment. The membrane was probed for the cleaved form of caspase-3 protein, and re-probed with an antibody directed to (total) actin to confirm equal loading (not shown). (h) Densitometric analyses: signals corresponding to cleaved caspase-3 were quantified and normalized against H_2O_2 alone (maximum). Each data point represents mean ± SE; n = 3.

but did attenuate the H_2O_2-induced cleavage of caspase-3 in HaCaT cells (Fig. S5), as we saw when we re-probed the left four lanes separately.

Discussion

We examined the effect of H_2O_2 and S1P in HaCaT cells. We found that S1P attenuated the H_2O_2-induced apoptosis in HaCaT cells, as assessed by the WST assay. Using TUNEL, it was found that H_2O_2 induced DNA fragmentation in HaCaT cells, and again, this was reduced by treatment with S1P. Our findings that S1P is able to counteract H_2O_2-dependent apoptotic responses of HaCaT cells are consistent with earlier reports suggesting that S1P could be a pro-survival sphingolipid metabolite. For example, S1P keeps keratinocyte cultures from undergoing apoptosis elicited by stimuli such as TNF-α[5] and UVB.[7] These earlier studies primarily focused on the roles of endogenous S1P. To our knowledge, the present report is the first to show antiapoptotic effects of exogenous S1P in HaCaT cells.

Caspase-3 is a key 'executor' protease of apoptotic processes of HaCaT cells.[15] We therefore examined the effects of H_2O_2 and/or S1P on caspase-3 by performing immunoblot analyses of HaCaT cells, using an antibody specific to the cleaved (activated) form of caspase-3. The H_2O_2-induced cleavage of caspase-3 protein was markedly reduced by preincubation with S1P.

The protein kinase Akt is a well-established antiapoptotic protein. It is one of the downstream effector proteins of the S1P receptor pathway, and stimulation of S1P receptors in keratinocytes leads to Akt activation.[11] Inhibitors ofAkt attenuate the antiapoptotic effects of Akt in keratinocytes.[16] Therefore, we evaluated the effects of H_2O_2 and/or S1P on Akt by assessing

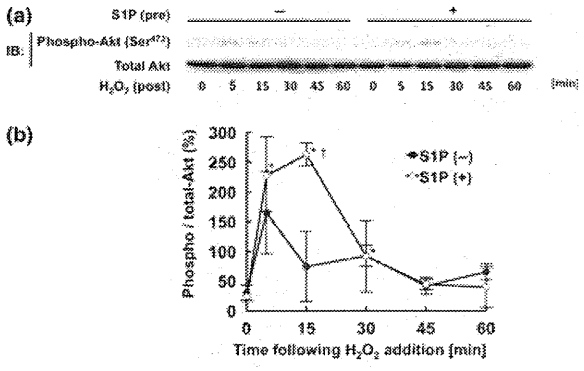

Figure 2 (a,b) Sphingosine 1-phosphate (S1P) pretreatment enhances H_2O_2-induced phosphorylation of Akt in HaCaT cells. HaCaT cells were pre-treated or not with S1P 1 μmol/L for 30 min, then treated with H_2O_2 1 mmol/L for the indicated times. (a) Equal amounts of protein (30 μg) were loaded per lane. (b) The resulting ratios of phospho-Akt to total Akt were then normalized to the basal value obtained in the absence of H_2O_2 and S1P. Each data point represents mean ± SE. Open and closed circles represent values obtained with and without pretreatment with S1P, respectively. $^*P < 0.05$ vs. 0 min, $^\dagger P < 0.05$ vs. S1P (–); $n = 7$.

the degrees of phosphorylation. The ratio of phosphorylated Akt at serine 473 was determined by using antibodies that recognize Akt and comparing the relative densitometry on immunoblots of activated Akt with the adjusted values of total Akt protein. Akt did not increase significantly with H_2O_2 alone, but did increase after pretreatment with S1P. Thus we sought to explore the roles of S1P receptors in our system.

We used a pharmacological inhibitor of PI3-K, wortmannin, to assess the effects of PI3-K inhibition. Pretreatment with this agent reduced S1P-induced phosphorylation of Akt and increased H_2O_2-evoked cleavage of caspase-3. In the presence of wortmannin, S1P was unable to prevent H_2O_2-elicited cleavage of caspase-3. These results indicate that the protective effects of S1P against H_2O_2-elicited apoptotic responses in HaCaT cells were mediated by the PI3-K/Akt pathway.

To explore the roles of S1P receptors in our system, we used RT-PCR in HaCaT cells, and detected transcripts encoding encoding $S1P_1$– $S1P_5$.

Recently, the therapeutic effects of S1P and S1P receptor-related agents have been assessed for certain condiions. For example, FTY720, which acts as an S1P receptor agonist when phosphorylated, has been used for the treatment of multiple sclerosis.[17] FTY720 also improved the degrees of contact hypersensitivity in a mouse model.[18] We investigated whether FTY720-P promotes H_2O_2-induced Akt phosphorylation. H_2O_2-elicited Akt phosphorylation was significantly enhanced when HaCaT cells were pretreated with FTY720-P, supporting the hypothesis that S1P attenuates H_2O_2-induced apoptosis as an S1P receptor agonist rather than as an intracellular second messenger.

We also assessed the effect of FTY720-P on Stat3, which is a mediator of H_2O_2-elicited cellular damage in normal human keratinocytes.[19] When HaCaT cells were pretreated with FTY720-P, the degree of serine 727 phosphorylation was reduced, but not that of tyrosine 705. Thus, Stat3 represents another potential

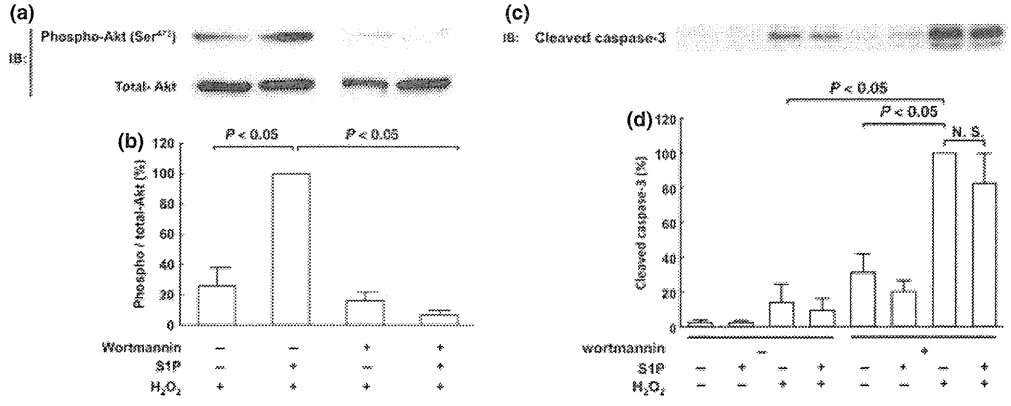

Figure 3 Wortmannin attenuates H_2O_2-induced phosphorylation of Akt and cleavage of caspase-3. (a,b) HaCaT cells were pretreated with wortmannin 10 nmol/L for 30 min, then treated with $H2O_2$ or vehicle (distilled water) for 15 min. (a) Equal amounts of protein (100 μg) were loaded per lane. and (b) analysed densitometrically. Data are expressed as means ± SE, $n = 3$. (c) HaCaT cells were pretreated with wortmannin 10 nmol/L for 30 min, then treated with S1P 1 μmol/L for 30 min, and the resulting membrane was probed for the cleaved form of caspase-3. (c) Equal amounts of protein (100 μg) were loaded per lane, and (d) analysed densitometrically. Data are expressed as means ± SE, $n = 4$. IB, immunoblot.

target of the S1P receptor system in H_2O_2-exposed HaCaT cells.

A wide array of other signalling proteins have been suggested as proximal molecules that connect cellular stimulation with execution of apoptosis. The MAPKs p38 and JNK have been previously implicated in oxidative stress-induced apoptosis in keratinocytes,[20] and we previously found that S1P protects cultured vascular endothelial cells from H_2O_2-induced apoptosis, associated with attenuation of p38 MAPK activation.[10] We therefore sought to explore whether S1P attenuates H_2O_2-induced apoptosis by modulating the activity of these molecules. We found that the MAPKs underwent robust phosphorylation (activation) responses. S1P did not affect the degree of phosphorylation of p38, JNK or ERK1/2 (data not shown). These results indicate that the PI3-K/Akt pathway may be more important than MAPKs in the anti-apoptotic effect of S1P in HaCaT cells.

In a previous study on vascular endothelial cells, H_2O_2 was shown to promote phosphorylation of Akt,[21] but in our study, we found that H_2O_2 by itself did not enhance phosphorylation of Akt in HaCaT cells. Schuppel *et al.* reported that high-dose (10 μmol/L) S1P attenuated phosphorylation of Akt in normal human keratinocytes[11]; however, we found that an increase of S1P from 1 to 10 μmol/L did not alter the degree of Akt phosphorylation in the presence of successively administered H_2O_2. The reason for this discrepancy is unknown. It may be due to the difference between HaCaT cells and primary keratinocytes. Nevertheless, our study suggests that a physiologically relevant concentration of S1P, i.e. 1 μmol/L, rather than pharmacological concentrations, seems to enhance phosphorylation of Akt. However, we used the concentration of 1 μmol/L because serum S1P concentrations seem to be within the range of several hundred nanomoles to a few micromoles in most (patho-)physiological conditions.[22] Our findings that the antiapoptotic effects of S1P act via phosphorylation of Akt are consistent with earlier reports showing that the PI3-K/Akt pathway is a major target of S1P in various cell types, including vascular endothelial cells.[23]

In our study, exogenously added S1P attenuated H_2O_2-elicited apoptotic responses in HaCaT cells, indicating the S1P receptors and the PI3K/Akt pathway as potential molecular targets of S1P-induced anti-apoptotic actions in these conditions. FTY720-P can also modulate cellular function by an S1P receptor-independent pathway.[24] Thus, although S1P receptor activation probably drives the PI3-K/Akt pathway, our results do not completely exclude the possibility that some of the effects of S1P are mediated in a receptor-independent fashion.

We propose that the antiapoptotic effects of S1P have potential clinical relevance, because H_2O_2 is derived from wound fluid,[8] and oxidative stress has a negative effect on wound healing via apoptosis of keratinocytes and vascular endothelial cells.[9] In an earlier study, we found that S1P attenuated oxidative stress-induced apoptosis in cultured endothelial cells.[10] The recent study by Kawanabe *et al.* provided the intriguing observation that addition of a high concentration of S1P had a therapeutic effect on wounded skin in diabetic, but not normal, mice.[25] Because our experiments were performed in HaCaT cells derived from humans, our data imply that S1P could also contribute to promotion of wound healing in humans.

Conclusion

S1P, a sphingolipid mediator, attenuates H_2O_2-induced apoptosis of HaCaT cells, via phosphorylation of Akt. S1P may have clinical relevance in a number of clinical conditions. Further investigations need to be performed to explore these interesting possibilities.

What's already known about this topic?

- In earlier studies, S1P was shown to prevent keratinocyte cultures from undergoing apoptosis elicited by stimuli such as TNF-α and UVB irradiation.
- These studies primarily focused on the roles of endogenous S1P.

What does this study add?

- To our knowledge, this is the first report of the anti-apoptotic effects of exogenous S1P in HaCaT cells.
- Our results demonstrate that the protective effects of S1P against H_2O_2-elicited apoptotic responses in HaCaT cells are mediated by the PI3-K/Akt pathway.
- S1P may be of use in a number of clinical conditions, including promotion of wound healing.

References

1 Hla T. Physiological and pathological actions of sphingosine 1-phosphate. *Semin Cell Dev Biol* 2004; **15**: 513–20.

2 Vogler R, Sauer B, Kim DS *et al.* Sphingosine-1-phosphate and its potentially paradoxical effects on critical parameters of cutaneous wound healing. *J Invest Dermatol* 2003; **120**: 693–700.

3 Kim DS, Kim SY, Kleuser B *et al.* Sphingosine-1-phosphate inhibits human keratinocyte proliferation via Akt/protein kinase B inactivation. *Cell Signal* 2004; **16**: 89–95.

4 Amano S, Akutsu N, Ogura Y *et al.* Increase of laminin 5 synthesis in human keratinocytes by acute wound fluid, inflammatory cytokines and growth factors, and lysophospholipids. *Br J Dermatol* 2004; **151**: 961–70.

5 Hammer S, Sauer B, Spika I *et al.* Glucocorticoids mediate differential anti-apoptotic effects in human fibroblasts and keratinocytes via sphingosine-1-phosphate formation. *J Cell Biochem* 2004; **91**: 840–51.

6 Manggau M, Kim DS, Ruwisch L *et al.* 1-Alpha,25-dihydroxyvitamin D3 protects human keratinocytes from apoptosis by the formation of sphingosine-1-phosphate. *J Invest Dermatol* 2001; **117**: 1241–9.

7 Uchida Y, Houben E, Park K *et al.* Hydrolytic pathway protects against ceramide-induced apoptosis in keratinocytes exposed to UVB. *J Invest Dermatol* 2010; **130**: 2472–80.

8 Roy S, Khanna S, Nallu K *et al.* Dermal wound healing is subject to redox control. *Mol Ther* 2006; **13**: 211–20.

9 Soneja A, Drews M, Malinski T. Role of nitric oxide, nitroxidative and oxidative stress in wound healing. *Pharmacol Report* 2005; **57**: 108–19.

10 Moriue T, Igarashi J, Yoneda K *et al.* Sphingosine 1-phosphate attenuates H2O2-induced apoptosis in endothelial cells. *Biochem Biophys Res Commun* 2008; **368**: 852–7.

11 Schuppel M, Kurschner U, Kleuser U *et al.* Sphingosine 1-phosphate restrains insulin-mediated keratinocyte proliferation via inhibition of Akt through the S1P2 receptor subtype. *J Invest Dermatol* 2008; **128**: 1747–56.

12 Boukamp P, Petrussevska RT, Breitkreutz D *et al.* Normal keratinization in a spontaneously immortalized aneuploid human keratinocyte cell line. *J Cell Biol* 1988; **106**: 761–71.

13 Yoneda K, Demitsu T, Nakai K *et al.* Activation of vascular endothelial growth factor receptor 2 in a cellular model of loricrin keratoderma. *J Biol Chem* 2010; **285**: 16184–94.

14 Igarashi J, Miyoshi M, Hashimoto T *et al.* Hydrogen peroxide induces S1P1 receptors and sensitizes vascular endothelial cells to sphingosine 1-phosphate, a platelet-derived lipid mediator. *Am J Physiol Cell Physiol* 2007; **292**: C740–8.

15 Shimizu H, Banno Y, Sumi N *et al.* Activation of p38 mitogen-activated protein kinase and caspases in UVB-induced apoptosis of human keratinocyte HaCaT cells. *J Invest Dermatol* 1999; **112**: 769–74.

16 Lewis DA, Hengeltraub SF, Gao FC *et al.* Aberrant NF-kappaB activity in HaCaT cells alters their response to UVB signaling. *J Invest Dermatol* 2006; **126**: 1885–92.

17 Chun J, Hartung HP. Mechanism of action of oral fingolimod (FTY720) in multiple sclerosis. *Clin Neuropharmacol* 2010; **33**: 91–101.

18 Sugita K, Kabashima K, Sakabe J *et al.* FTY720 regulates bone marrow egress of eosinophils and modulates late-phase skin reaction in mice. *Am J Pathol* 2010; **177**: 1881–7.

19 Bito T, Izu K, Tokura Y. Evaluation of toxicity and Stat3 activation induced by hydrogen peroxide exposure to the skin in healthy individuals. *J Dermatol Sci* 2010; **58**: 157–9.

20 Diker-Cohen T, Koren R, Ravid A. Programmed cell death of stressed keratinocytes and its inhibition by vitamin D. the role of death and survival signaling pathways. *Apoptosis* 2006; **11**: 519–34.

21 Yang B, Oo TN, Rizzo V. Lipid rafts mediate H_2O_2 prosurvival effects in cultured endothelial cells. *FASEB J* 2006; **20**: 1501–3.

22 Yatomi Y, Igarashi Y, Yang L *et al.* Sphingosine 1-phosphate, a bioactive sphingolipid abundantly stored in platelets, is a normal constituent of human plasma and serum. *J Biochem* 1997; **121**: 969–73.

23 Igarashi J, Bernier SG, Michel T. Sphingosine 1-phosphate and activation of endothelial nitric-oxide synthase. differential regulation of Akt and MAP kinase pathways by EDG and bradykinin receptors in vascular endothelial cells. *J Biol Chem* 2001; **276**: 12420–6.

24 Halin C, Scimone ML, Bonasio R *et al.* The S1P-analog FTY720 differentially modulates T-cell homing via HEV. T-cell-expressed S1P1 amplifies integrin activation in peripheral lymph nodes but not in Peyer patches. *Blood* 2005; **106**: 1314–22.

25 Kawanabe T, Kawakami T, Yatomi Y *et al.* Sphingosine 1-phosphate accelerates wound healing in diabetic mice. *J Dermatol Sci* 2007; **48**: 53–60.

Supporting Information

Additional Supporting Information may be found in the online version of this article:

Figure S1. Reverse transcription (RT)-PCR analysis of mRNA encoding S1P receptors in HaCaT cells.

Figure S2. FTY720-P pretreatment enhanced H_2O_2-induced phosphorylation of Akt in HaCaT cells.

Figure S3. FTY720-P pretreatment modulates H_2O_2-induced phosphorylation of signal transducer and activator of transcription (Stat)3 in HaCaT cells.

Figure S4. Pretreatment with higher dose of sphingosine 1-phosphate (S1P) did not attenuate H_2O_2-induced phosphorylation of Akt in HaCaT cells.

Figure S5. Sphingosine 1-phosphate (S1P) pretreatment attenuated the H_2O_2-induced cleavage of caspase-3 in HaCaT cells.

Table S1. Primers used for reverse transcription (RT)-PCR analysis.